

# **ELECTROLYTE DESIGN FOR QUASI-SOLID-STATE LITHIUM-SULFUR BATTERIES**

**Marzhan Aliyakbarova, BSc**

**Submitted in fulfilment of the requirements  
for the degree of Master of Science  
in Chemical Engineering**



**NAZARBAYEV  
UNIVERSITY**

**School of Engineering  
Department of Chemical & Materials Engineering  
Nazarbayev University**

**53 Kabanbay Batyr Avenue,  
Astana, Kazakhstan, 010000  
Supervisors: Prof. Z. Bakenov,  
Dr. A. Belgibayeva**

**13<sup>th</sup> May 2025**

## DECLARATION

I hereby, declare that this manuscript, entitled "*Electrolyte design for quasi-solid-state lithium-sulfur batteries*", is the result of my own work except for quotations and citations which have been duly acknowledged.

I also declare that, to the best of my knowledge and belief, it has not been previously or concurrently submitted, in whole or in part, for any other degree or diploma at Nazarbayev University or any other national or international institution.



-----  
Name: Marzhan Aliyakbarova

Date: 13.05.2025

# Acknowledgements

This study was conducted under the Program Targeted Funding BR21882402, “Development of new technologies of materials and energy storage systems for a green economy” by the Ministry of Science and Higher Education of the Republic of Kazakhstan. The Supervisor of my thesis and the Principal Investigator of the Program is Professor of Chemical and Materials Engineering Department, the Academician of the National Academy of Science of Kazakhstan under the President of the Republic of Kazakhstan Zhumabay Bakenov and the Co-Principal Investigator is a Leading Researcher of National Laboratory Astana, Dr. Aliya Mukanova. The co-supervisor is a Leading Researcher of National Laboratory Astana Dr. Ayaulym Belgibayeva.

To start with, I would like to express my immense gratitude to Professor Zhumabay Bakenov, Dr. Aliya Mukanova, and Dr. Ayaulym Belgibayeva for leading my research pathway, endless support, invaluable insights and encouragement throughout the process of writing this thesis.

I also would like to thank my colleagues Mukagali Yegamkulov, Assel Serikkazyeva, Nurbolat Issatayev, Altynay Zhumabekova, and Akbota Kelgenbayeva, who have supported and encouraged me along this way. I would like to thank the whole Battery Group research members for the opportunity to work in such a friendly environment.

I would also highly appreciate the support and patience of my family and friends during these two years.

Last but not least, I am deeply grateful to Nazarbayev University for providing me with remarkable knowledge, highly valuable experience, and a chance to join the NU community.

# Table of Contents

<b><u>Declaration</u></b> .....	2
<b><u>Acknowledgements</u></b> .....	3
<b><u>List of Abbreviations</u></b> .....	6
<b><u>List of figures</u></b> .....	8
<b><u>List of tables</u></b> .....	10
<b><u>Abstract</u></b> .....	11
<b><u>Chapter 1 - Introduction</u></b> .....	12
<u>1.1 General overview</u> .....	12
<u>1.2 Research objectives</u> .....	13
<u>1.3 Research Novelty</u> .....	13
<u>1.4 Comparison of QSSE and other electrolytes</u> .....	13
<u>1.5 Thesis overview</u> .....	13
<b><u>Chapter 2- Literature review</u></b> .....	15
<u>2.1 Introduction to QSSLBs</u> .....	15
<u>2.2 Choice of QSSE components</u> .....	17
<u>2.3 Comparison of QSSE preparation methods</u> .....	18
<u>2.3.1 In-situ polymerization</u> .....	18
<u>2.3.2 Solution casting</u> .....	21
<u>2.3.3 Phase inversion</u> .....	26
<u>2.3.4 Electrospinning</u> .....	27
<b><u>Chapter 3 - Experimental section</u></b> .....	32
<u>3.1 Materials</u> .....	32
<u>3.2 Preparation of PE</u> .....	32
<u>3.2.1 Electrospinning technique</u> .....	32
<u>3.2.2 Solution casting technique</u> .....	32
<u>3.2.3 Spin coating technique</u> .....	32
<u>3.3 Physical characterizations</u> .....	33
<u>3.4 PEIS analysis</u> .....	33
<b><u>Chapter 4 - Results and discussion</u></b> .....	34
<u>4.1 Effect of LITFSI concentration on the physical properties of QSSE prepared by electrospinning</u> .....	34
<u>4.2 Effect of preparation method on the physical properties of QSSE</u> .....	35
<u>4.3 Comparison with literature reported QSSEs</u> .....	42
<b><u>Chapter 5 - Conclusions</u></b> .....	43

**Bibliography**..... 44

# List of abbreviations

AM	Active material
ASSLSBs	All-solid-state lithium-sulfur batteries
CA	Cellulose acetate
COF	covalent organic framework
COF-SH	sulfhydryl and imine-functionalized covalent organic framework
CSE	composite solid electrolyte
DLHSE	double-layer hybrid solid electrolyte
DMF	dimethylformamide
DOL	1,3-dioxolane
E/S ratio	electrolyte-to-sulfur ratio
FTIR	Fourier transform infra-red spectroscopy
GF-LE	glass fiber-liquid electrolyte
GPE	gel polymer electrolyte
IDCN	integrated, dynamic cross-linked polymer network
LAGP	lithium aluminum germanium phosphate
LATP	Lithium Lanthanum Titanate Phosphate
LE	liquid electrolyte
LFP	LiFePO <sub>4</sub>
LIB	Lithium ion batteries
LiTFSI	lithium bis(trifluoromethylsulphonyl)imide
LLZO	lithium lanthanum zirconium oxide
LLZTO	lithium lanthanum tantalum zirconate
LMA	lithium metal anode
LSBs	lithium-sulfur batteries
LTPO-HSE	LiTa <sub>2</sub> PO <sub>8</sub> Hybrid-solid electrolyte
NASICON	Sodium super ionic conductor
PAN	Polyacrylonitrile
PDOL	Poly Dioxolane
PE	Polymer electrolyte
PEO	Poly (ethylene oxide)
PMMA	Poly (methyl methacrylate)
PVDF	Polyvinylidene fluoride
PVDF-HFP	Polyvinylidene fluoride-co-hexafluoropropylene

PVP	polyvinylpyrrolidone
Py <sub>14</sub> TFSI	1-butyl-1-methyl pyrrolidinium bis-trifluoromethanesulfonimide
QSSE	quasi-solid-state-electrolyte
QSSLBs	quasi-solid-state lithium-sulfur batteries
SEIS	solid electrolyte interface layer
SEM	scanning electron microscopy
SSP	spherical star polymer
TEGDN	triethylene glycol dinitrate

# List of figures

Figure 1. Schematic of conventional LSBs, QSSLBs and ASSLSBs.....	15
Figure 2. Illustration of (a) IDCN, (b) illustration of IDCN at nanoscale, (c) illustration of IDCN at molecular scale.....	18
Figure 3. (a) Graphical illustration obtaining in-situ polymerized PDOL-SiCl <sub>4</sub> -SiO <sub>2</sub> , (b) Li/PDOL-SiCl <sub>4</sub> -SiO <sub>2</sub> /Li cell's Nyquist plot before and after polarization, (c) SEM image of PDOL-SiCl <sub>4</sub> -SiO <sub>2</sub> before polymerization.....	18
Figure 4. A drafted illustration of LSB with lean and liquid electrolyte with (a) LE and (b) PE.....	19
Figure 5. Schematic diagram of (a) the LMA with N-poor SEI, (b) LMA with N-rich SEI.	19
Figure 6. SEM images of LMA from QSSE battery (a) without and (b) with TEGDN after charge/discharge process.....	20
Figure 7. (a) Impact of various additives on the conductivity of LiTFSI/ Py <sub>14</sub> TFSI/ CA/ PVDF electrolytes; (b) dependance of ionic conductivity on LiTFSI weight and tensile strength of LiTFSI/Py <sub>14</sub> TFSI/CA/PVDF electrolytes.....	22
Figure 8. Visual presentation of producing PE by solvent casting method.....	23
Figure 9. Nyquist plot of influence of LLZTO diameter on resistance of CSE.....	24
Figure 10. Visual representation of PVDF-HFP/ LiTFSI/LLZTO electrolyte processing ...	24
Figure 11. Visual representation of DLHSE fabrication.....	26
Figure 12. SEM images of (a) PVDF-HFP, LiTFSI prepared via electrospinning, (b) PVDF-HFP, LiTFSI, f-SiO <sub>2</sub> prepared via electrospinning, (c) PVDF-HFP, LiTFSI, nm-SiO <sub>2</sub> prepared via electrospinning, and (d) PVDF-HFP, LiTFSI, nm-TiO <sub>2</sub> prepared via electrospinning.....	28
Figure 13. Nyquist plots of the GPE (a) before cycling and (b) after 10 cycles.....	28
Figure 14. Schematic representation of coin cell assembling for PEIS analysis.....	32
Figure 15. SEM images of samples prepared via electrospinning with (a) 0%, (b) 1%, (c) 3%, (d) 5%, (e) 7%, (f) 10%, and (g) 16% LiTFSI.....	33
Figure 16. Cross-sectional SEM images of samples prepared via electrospinning with (a) 0%, (b) 1%, (c) 3%, (d) 5%, (e) 7%, (f) 10%, and (g) 16% LiTFSI.....	34
Figure 17. Nyquist plot of samples (a) 0%, (b) 1%, (c) 3%, (d) 5%, (e) 7%, (f) 10%, and (g) 16% LiTFSI prepared via electrospinning.....	34
Figure 18. XRD analysis of 5% LiTFSI sample prepared by electrospinning, solution casting,	36

and spin coating.....	
Figure 19. FTIR spectra of 5% LiTFSI sample prepared by electrospinning, solution casting, and spin coating.....	37
Figure 20. SEM-EDS characterization of 5% LiTFSI produced via (a) electrospinning, (b) solution casting, and (c) spin coating.....	38
Figure 21. 5% LiTFSI samples (a) before and (b) after heat treatment.....	39
Figure 22. Cross-sectional SEM characterization of 5% LiTFSI produced via (a) solution casting, and (b) spin coating. ....	39
Figure 23. Nyquist plots of 5% LiTFSI prepared by (a) solution casting (b) spin coating....	40

## List of Tables

Table 1. Comparison of LTPO-HSE, GF-LE QSSEs.	21
Table 2. The benefits and drawbacks of QSSE fabrication methods	30
Table 3. Ionic conductivity of PE obtained via electrospinning.	35
Table 4. Ionic conductivity of 5% LiTFSI obtained via solution casting and spin coating approaches.	40

# Abstract

This study investigates the creation and characterization of quasi-solid-state electrolytes (QSSEs) for lithium-sulfur batteries (LSBs), with a focus on improving ionic conductivity. The research started conducting literature review with a highlight of QSSE preparation techniques. For the creation of polymer electrolytes (PEs) based on polyvinylidene fluoride-co-hexafluoropropylene (PVDF-HFP) and lithium bis(trifluoromethylsulphonyl)imide (LiTFSI), the study optimizes the LiTFSI content. Moreover, this study compares three widely used preparation methods, including electrospinning, solution casting, and spin coating. The scanning electron microscopy coupled with energy dispersive X-ray spectroscopy (SEM-EDS), Fourier-transform infrared spectroscopy (FTIR), X-ray diffraction (XRD), potentiostatic electrochemical impedance spectroscopy (PEIS) and thermal stability analyses were done to investigate morphology, composition, ionic conductivity, and thermal characteristics of the produced electrolytes. According to XRD analysis shows that preparation method affects the crystallinity of the resulting PE. Concurrently FTIR shows modest crystallinity and strong ion-polymer interaction of electrospun sample, which makes electrospinning technique more favorable for efficient ion transport in PEs. Moreover, the PEIS analysis confirms that electrospinning greatly enhances the PE's ionic conductivity.

# Chapter 1- Introduction

## 1.1 General overview

Kazakhstan's extensive natural resources make it an ideal site for the development of novel battery technologies. This shift toward a green economy is critical for solving global concerns such as climate change, resource depletion, and environmental contamination. Utilizing local resources for battery manufacture is critical to Kazakhstan's economic growth, industrial sector, sustainable energy movement, and environmental sustainability. This strategy will considerably improve the efficiency of natural resource utilization while reducing negative environmental consequences.

According to the Ministry of Energy, the sulfur level of domestic oil fluctuates between 0.35% and 1.69%. Tengizchevroil, a joint venture, currently produces nearly all of Kazakhstan's sulfur, up to 1.6 million tons per year and this amount is planned to increase to 2.2 million tons after Tengizchevroil's expansion [1]. Sulfur is the primary component of lithium-sulfur batteries (LSBs), which are one of the "hot" areas of battery development across the world [2-4].

LSBs are a promising energy storage technology that has meet notable scientific observation lately [2-4].

LSBs have great potential for their high energy density and cost-effectiveness in energy storage, making them perfect candidates for next-generation portable and sustainable energy solutions [2]. Sulfur has a high theoretical capacity of 1675 mAh/g and an energy density of 2600 Wh/kg. Furthermore, the abundance of sulfur in nature and its inexpensive cost make LSBs more desirable [2].

The main electrochemical reaction in LSBs can be written like:  $S_8 + 16Li \leftrightarrow 8Li_2S$ . But sulfur undergoes several step reactions which will create compounds called polysulfides  $Li_2S_n$  where the  $n$  varies from 2 to 8. During the charge-discharge process, long-chain polysulfides  $Li_2S_n$  ( $4 < n \leq 8$ ) turn into short-chain polysulfides  $Li_2S_n$ , ( $2 < n \leq 4$ ), then eventually  $Li_2S_2$  and  $Li_2S$  are composed.

On the other hand, low electrical conductivity of sulfur and its lithiated products, polysulfide dissolution in electrolyte causing the shuttle effect (phenomenon of diffusion of polysulfides to the anode side), and considerable volume changes during cycling result in rapid capacity degradation and short cycle life of LSBs [4,5].

One of the approaches for restricting the dissolution and shuttle of polysulfides is reducing the amount of liquid electrolyte (LE) [2]. In this regard, quasi-solid-state electrolyte (QSSE) with a minimal amount of LE is considered as an appealing solution [2].

## 1.2 Research objectives

The objective of this work is to emerge a QSSE with elevated ionic conductivity, and small interfacial resistance, which is crucial for lithium transfer, and also to obtain a layer with proper mechanical stability that could prevent polysulfide dissolution into the electrolyte and proscribe the polysulfide shuttling. Thus, this project aims to acquire the electrolyte layer with low activation energy at room temperature, lithium transference number close to one, minor electronic conductivity, a large potential stability window, and good chemical compatibility with both positive and negative electrodes.

## 1.3 Research Novelty

The novelty of this work is to develop QSSE made of polyvinylidene fluoride-co-hexafluoropropylene (PVDF-HFP) / lithium bis(trifluoromethylsulphonyl)imide (LiTFSI) with high ionic conductivity and compare three frequently used techniques used in QSSE fabrication. This configuration would greatly decrease the "shuttle" effect and volumetric expansion of the cathode while maintaining mechanical flexibility, hence drastically increasing the electrochemical characteristics and stability of sulfur cells.

## 1.4 Comparison of QSSE and other electrolytes

Electrolyte is the necessary part of batteries, which is responsible for the ion transport between cathode and anode. The traditional batteries with LE have several pros, as elevated ionic conductivity and effective electrode wetting, which will influence the effective use of active material (AM) [6]. Nevertheless, the exhibition of lithium dendrites, the shuttle effect, the toxicity of LE components, problems with leakage, high flammability, and high self-discharge rates can be considered as cons of LSBs with LE [7,8]. Regarding the safety and prevention of the shuttle effect, a favorable option is to get rid of LE and assemble all solid-state batteries. However, all-solid-state lithium-sulfur batteries (ASSLSBs) have high interfacial resistance between the components, which will lead to low ionic conductivity and limit their application in real life [9]. QSSEs offer an optimal balance between liquid and solid electrolytes, combining high ionic conductivity with effective lithium dendrite suppression [10]. The flexibility of polymer should enhance the interfacial contact and positively affect the electrochemical performance of the whole battery; minimizing the amount of LE will improve the safety.

## 1.5 Thesis overview

Chapter 1 introduces the LSBs, operation mechanism and parts as well as the main strength and weaknesses of LSBs. This section covers the objectives, novelty and importance of research

topic. It also includes the work motivation, main goals and provides a brief synopsis of each chapter of this thesis.

Chapter 2 introduces QSSE and provides QSSE's outweighs in comparison to all solid and traditional batteries with LE. Moreover, it includes review about the existing methods of obtaining QSSE as in-situ polymerization, solution casting, phase inversion and electrospinning. Also, the justification of chosen methods and compounds to prepare QSSE is provided in this section.

Chapter 3 covers the experimental part of producing polymer material via electrospinning, solution casting and spin coating methods. Additionally, information about sample preparation to analysis and parameters of physical characterization: Fourier-transform infrared spectroscopy (FTIR), X-ray diffraction (XRD), scanning electron microscopy coupled with energy dispersive X-ray spectroscopy (SEM-EDS) and potentiostatic electrochemical impedance spectroscopy (PEIS) analysis reported in Chapter 3.

Chapter 4 provides the outcome of experiments and discusses research findings such as the ionic conductivity, morphology of samples, and degree of crystallization.

Chapter 5 reports the outcome of research, as well as the future work that needs to be completed and contribution of author to research article.

# Chapter 2- Literature review

## 2.1 Introduction to QSSLBs

LSBs have their own advantages and a number of disadvantages. One of the cons is that both sulfur and the product of the interaction with lithium  $\text{Li}_2\text{S}$ , are electrically insulating, resulting in low AM utilization and poor cycle performance [11]. Furthermore, the volume-changing features can contribute to low AM usage and reduced interfacial contact between cell components [2]. There's also the shuttling impact to consider. The shuttle effect occurs when intermediate products of the electrochemical reactions, high-order lithium polysulfides, diffuse toward lithium metal while low-order polysulfides diffuse backward in an ether-based electrolyte [2]. Shuttling causes low coulombic efficiency (CE), rapid self-discharging rates, and poor cycle performance [12].

To overcome the hurdles associated with the shuttling effect, the use of QSSE is regarded as the best solution due to the enhanced ionic conductivity, exceptional contact between inner parts of the cell, and promoted safety. Thus, the problems of sulfur-containing cathodes can be solved by using QSSE.

A quasi-solid-state lithium-sulfur battery (QSSLB) is made up of metallic lithium, a sulfur-based positive electrode, a polymer matrix with lithium salt, and a small amount of LE. Conventional and QSSLBs work on similar principles [13-15]. The ion conduction in QSSLBs is explained by the effect of the electric field. The electric field affects the migrating polymer groups, which will ensure the ion conduction [16].

While QSSLBs show considerable promise, they must overcome several challenges before becoming economically feasible, including increased energy density, cycle life, and rate capability. Ongoing research tries to address these issues by innovative material design, interface engineering, and cell-level optimization [13, 16]. Figure 1 depicts that QSSLBs can be considered as an encouraging analog of ASSLSBs with several advantages: higher ionic conductivity, better interfacial contact, and a high level of safety [2].

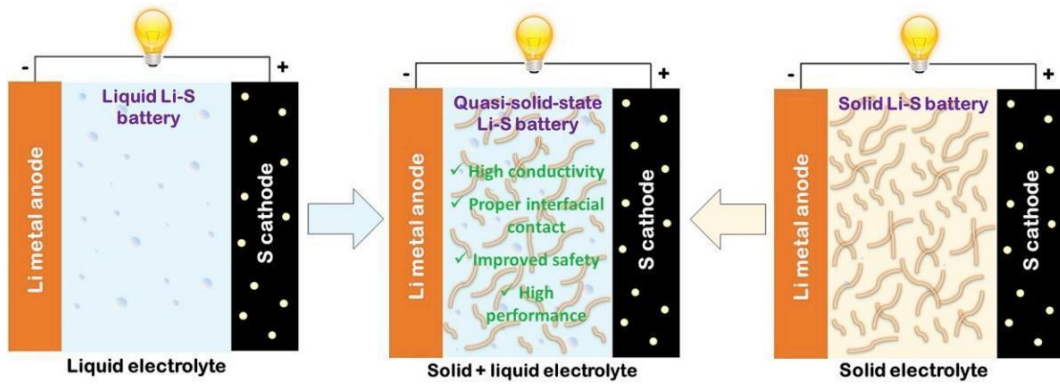


Figure 1. Schematic of conventional LSBs, QSSLBs and ASSLSBs [2].

With the great advantages of QSSE they also exhibit some limitations, such as polysulfide dissolution; lithium dendrite formation; lower mechanical, electrical and thermal stability, and limited cycle life.

QSSEs do not completely stop lithium polysulfides from dissolving into the electrolyte, despite advancements [17]. The polysulfide shuttle effect, in which polysulfides move across electrodes and cause self-discharge and capacity loss, is brought on by this disintegration. Since liquid components in QSSEs may aid in the dissolving of polysulfides, their presence may make this problem worse. The creation of QSSEs with improved polysulfide retention capacities is necessary to meet this problem.

QSSEs are less successful than all-solid-state electrolytes at preventing the production of lithium dendrites, while having better mechanical stability than LEs. Dendrites have the ability to pierce the electrolyte, limiting battery longevity and safety by generating internal short circuits [10]. Because of the liquid components in their structure, QSSEs frequently have limited thermal stability and electrochemical stability windows. These restrictions may cause electrolyte breakdown at elevated temperatures and voltages, which might compromise battery safety and performance. For practical use, QSSEs with enhanced thermal stability and wider electrochemical stability windows must be developed.

Liquid plasticizers are usually required to achieve high ionic conductivity in QSSEs, which may weaken the electrolyte's mechanical strength. This trade-off has an influence on the battery's overall performance and lifetime, making it challenging to achieve a balance between conductivity and structural integrity. To get the ideal balance between conductivity and mechanical stability, research is being done to optimize the composition of QSSEs.

Poor interfacial contact between QSSEs and electrodes can result in higher interfacial resistance and worse battery performance. This problem is most noticeable at the lithium metal anode, where dendritic growth and uneven lithium deposition can be caused by interfacial

instability. To overcome this difficulty, surface alterations and sophisticated electrolyte formulations must be used to increase interfacial compatibility.

Complex procedures including in-situ polymerization and the addition of different additives are frequently used in the manufacture of QSSEs and scaling them up for commercial production can be difficult. In order to make QSSEs commercially viable, it is crucial to streamline the production procedures and guarantee their scalability [18].

## 2.2 Choice of QSSE components

Several polymers have been investigated as host matrices in QSSEs, including poly (ethylene oxide) (PEO), poly (methyl methacrylate) (PMMA), polyacrylonitrile (PAN), poly(dioxolane) (PDOL), and PVDF-HFP, each with unique advantages and limitations. PEO, while well investigated for its strong lithium salt solvating capacity, has a high crystallinity, which limits ionic mobility at ambient temperature [19]. PMMA and PAN have excellent electrochemical stability and mechanical strength, but they require plasticizers or fillers to obtain adequate ionic conductivity [20,21]. PDOL, a new entrant, has good room-temperature conductivity due to its amorphous, ether-rich structure, but it struggles with oxidative stability at higher voltages [22]. PVDF-HFP, on the other hand, is notable for its distinct property balance.

PVDF-HFP is made via copolymerization of vinylidene fluoride and hexafluoropropylene and consists of two phases: crystalline and amorphous. Amorphous part of the polymer assists in lithium ion transport and yields high ionic conductivity [23]. Also, PVDF-HFP provides proper mechanical properties to electrolyte and flexibility to ensure good contact between electrolyte and electrode [24-25]. Moreover, PVDF-HFP exhibits high dielectric constant resulting in easy dissociation of lithium ions from salts [24]. Good thermal stability and low glass transition temperature, compatibility with lithium salts and metallic lithium makes PVDF-HFP the best component of polymer electrolytes (PEs) [25].

LiTFSI helps PEs have strong ionic conductivity, which is necessary for effective battery operation. LiTFSI-containing electrolytes According to studies LiTFSI-containing electrolytes have advantageous ionic conductivity values, which promote effective lithium-ion transport [26].

LiTFSI-based electrolytes are appropriate for high-voltage applications because of their wide electrochemical stability window. According to research, LiTFSI-containing electrolytes may remain stable at voltages of about 4 V, which is advantageous for battery performance.

The production of electrolytes with desired characteristics is made possible by LiTFSI's solubility in a variety of organic solvents. It has been demonstrated that combining LiTFSI with solvents such as ethylene carbonate produces electrolytes with balanced transport and thermal characteristics, which helps to provide good cycle stability in lithium-ion batteries (LIBs).

The thermal stability of LiTFSI-based electrolytes is essential for battery performance and safety. According to studies, electrolytes with LiTFSI- lithium difluoro(oxalato)borate dual-salts exhibit noticeably higher thermal stability than those with LiPF<sub>6</sub>, indicating that LiTFSI helps to improve electrolyte thermal stability [27].

High lithium-ion transference numbers and low ionic pairing are characteristics of LiTFSI-based electrolytes that are advantageous for effective battery operation. Studies have demonstrated that electrolytes containing LiTFSI and LiNO<sub>3</sub> as co-salts have high lithium-ion transference numbers and ionic conductivity, which improve battery performance [28].

High compatibility between LiTFSI-based electrolytes and lithium metal anodes lowers the possibility of dendritic development. LiTFSI-containing electrolytes have been shown to have high compatibility with lithium metal, which enhances the stability and security of LIBs [29].

### 2.3 Comparison of QSSE preparation methods

There are several techniques of developing QSSE for the batteries: in-situ polymerization, electrospinning, solution casting, phase inversion, etc.

#### 2.3.1 In-situ polymerization

In-situ polymerization is a process of obtaining solid electrolyte at the surface of the electrode. Procedure starts with preparing homogeneous mixture of monomer and lithium salts, subsequently mixture injected into the assembled battery. Afterwards, the battery was cured by light or heat to create a solid electrolyte [30].

A typical in-situ polymerization technique occurs between two monomers with an ability to polymerize. The monomers solution mixed and via adding initiator polymerization occurs. In the case of obtaining QSSE there were cases that only half of one monomer polymerizes and the left stays as LE [31].

Usually, crystalline polymer chains have a low concentration of segmental motion; researchers get rid of this problem by adding liquid or solid plasticizers [32, 33]. Liquid plasticizers with low melting points could have improved the ion transport by excellent ability to solvate. Usually, QSSE with high ionic conductivity is obtained when the mass ratio of liquid content is higher than 50%, while in this work the amount of LE is only 8  $\mu\text{l}$  which corresponds to 10% of the whole mass of QSSE. Elevated ionic conductivity ( $2.96 \times 10^{-4} \text{ S cm}^{-1}$ ) and immense Li<sup>+</sup> transference number (0.81) are reached by developing an amorphous, integrated, dynamic cross-linked polymer network (IDCN). IDCN is made of spherical star polymer (SSP) and Poly-dioxolane (PDOL) is depicted in Figure 2. SSP, which plays a role of solid plasticizer, consists of hyperbranched poly-3-hydroxymethyl-3'-methyloxetane and PDOL [33].

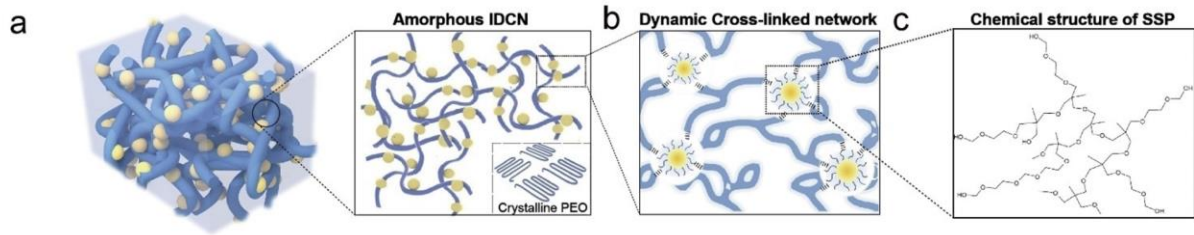


Figure 2. Illustration of (a) IDCN, (b) illustration of IDCN at nanoscale, (c) illustration of IDCN at molecular scale [33].

In the study by Hu et al, gel consists of several compounds, including  $\text{SiO}_2$ , dioxolane (DOL), and  $\text{SiCl}_4$  [34].  $\text{SiCl}_4$  is utilized as initiator of ring-opening polymerization of DOL and also contributes to the composing of the solid electrolyte interface (SEI) layer. Figure 3a shows the mechanism of ring-opening polymerization and in-situ polymerization process. Figure 3c depicts the gel polymer electrolyte (GPE) composed of  $\text{SiO}_2$ , DOL,  $\text{SiCl}_4$  before and after polymerization. According to the Nyquist plot (Figure 3 b), the ionic conductivity of GPE was equal to  $5.37 \times 10^{-4} \text{ S cm}^{-1}$ .

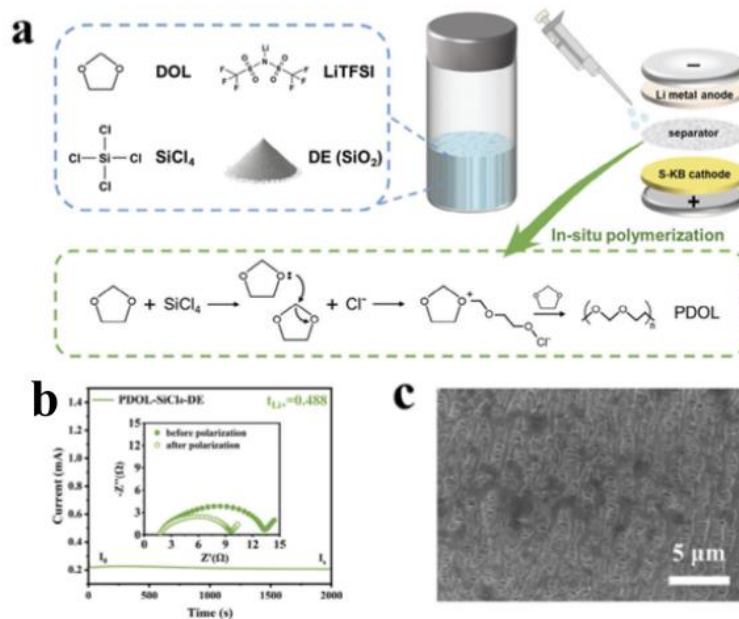


Figure 3. Graphical illustration obtaining in-situ polymerized PDOL-SiCl<sub>4</sub>-SiO<sub>2</sub>, (b) Li/PDOL-SiCl<sub>4</sub>-SiO<sub>2</sub>/Li cell's Nyquist plot before and after polarization, (c) SEM image of PDOL-SiCl<sub>4</sub>-SiO<sub>2</sub> before polymerization [34].

Another initiator of polymerization of DOL was introduced in a study by Liao et al [35]. Strong Lewis acids, such as (pentafluorophenyl)boron -  $\text{B}(\text{C}_6\text{F}_5)_3$ , can interact with oxygen atoms in molecule of polymer. It causes the reduced electron density of the bond between C-O in DOL.

So, the ring opening will be exhibited easily [40]. The main novelty of this work is utilizing in situ polymerized lean electrolyte, which will ensure the even arrangement of electrolyte (Figure 4b); meanwhile utilizing the cell with LE could have inappropriate distribution. The ionic conductivity of QSSE was  $2.9 \times 10^{-4} \text{ S cm}^{-1}$ .

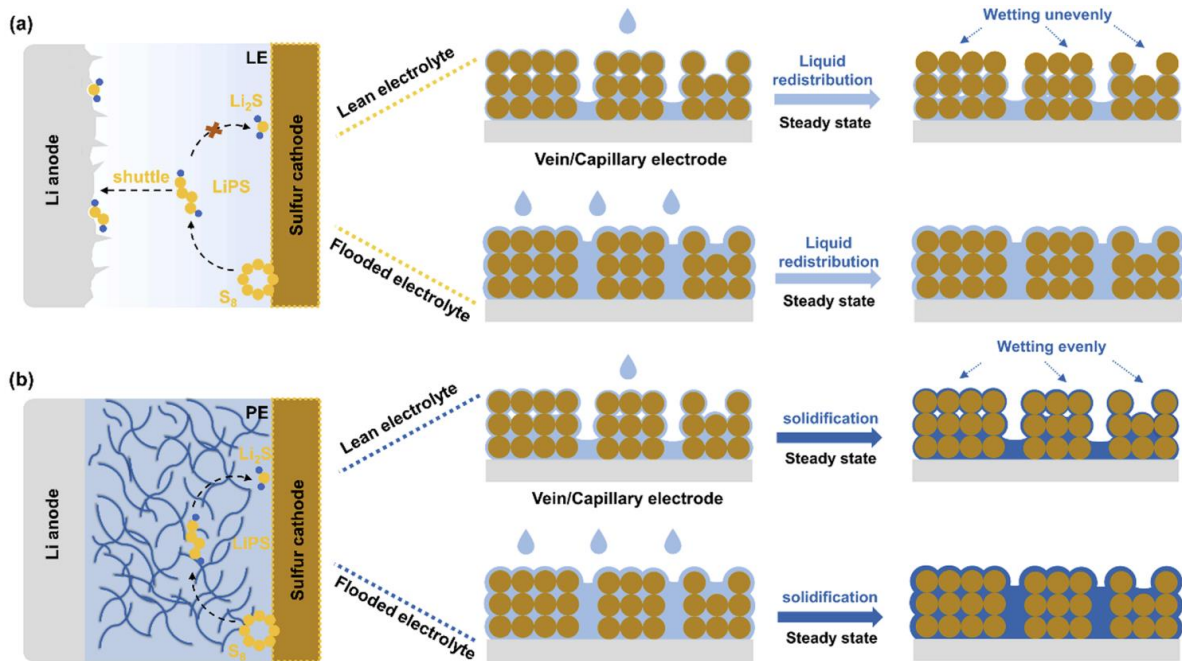


Figure 4. A drafted illustration of LSB with lean and liquid electrolyte with (a) LE and (b) PE [40].

$\text{LiNO}_3$  is usually applied as the component of LE for LIBs due to improving the ability to form a SEI layer. However,  $\text{LiNO}_3$  can terminate the polymerization of DOL. So, in the next study, triethylene glycol dinitrate (TEGDN) is used as an analogue of  $\text{LiNO}_3$  which will also create an excellent SEI layer but will not block the process of in-situ polymerization [36]. The schematic illustration of QSSE with TEGDN is shown in Figure 5.

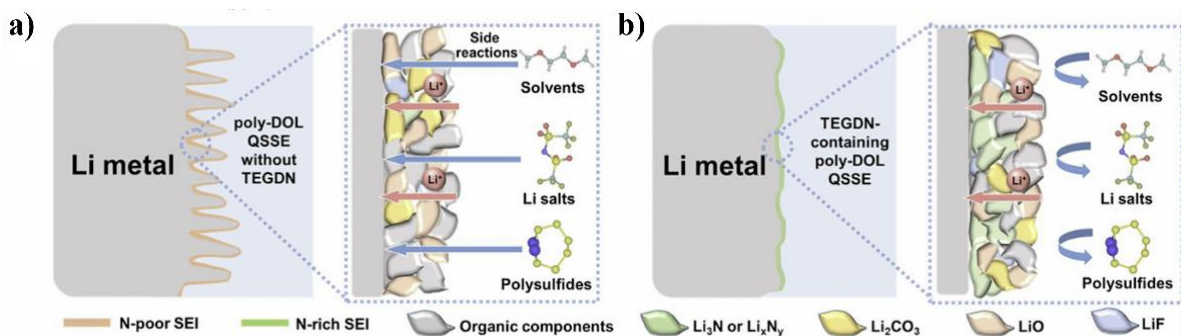


Figure 5. Schematic diagram of (a) the LMA with N-poor SEI, (b) LMA with N-rich SEI [36].

Researchers have proven their idea using scanning electron microscopy (SEM) images (Figure 6a). The sample without TEGDN and Figure 6e with the TEGDN layer, it can be seen that the lithium metal anode without the layer has undergone several parasitic reactions and changed sufficiently.

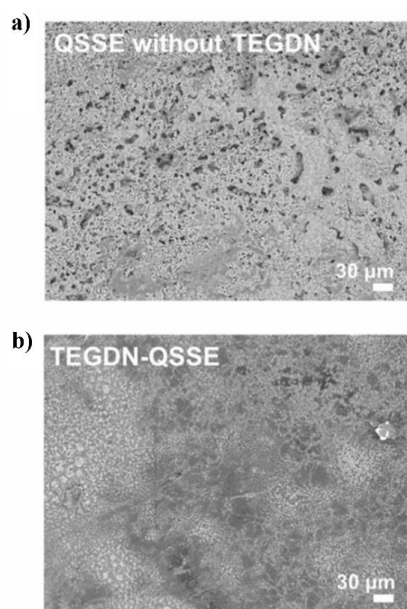


Figure 6. SEM images of LMA from QSSE battery (a) without and (b) with TEGDN after charge/discharge process [36].

Overall, the in-situ polymerization enhances the interface contact within the battery parts. This positively effects on ionic conductivity (till  $5.37 \times 10^{-4} \text{ S cm}^{-1}$ ) and  $\text{Li}^+$  transference number (0.81). However, the difficulty of controlling the amount of liquid and possibility of side reactions interfere with the application of this technique.

### 2.3.2 Solution casting

Solution casting is a technique where the liquid mixture of polymer and solvent is applied onto the flat surface and dried to dispose of the liquid solvent.

To produce the solid part of QSSE, PVDF-HFP and succinonitrile were mixed into a thick solution using dimethylformamide (DMF) as solvent, after that LiTFSI salt was added and left for 6 h and  $65^\circ\text{C}$ . Subsequently,  $\text{LiTa}_2\text{PO}_8$  was introduced to the solution; the whole process of obtaining a homogeneous solution takes 10 h. The solution was cast on glass and dried at  $60^\circ\text{C}$ . According to the Nyquist plot, the ionic conductivity of the QSSE was  $10^{-3} \text{ S cm}^{-1}$ .

The microcalorimetric measurements have revealed that heat generation of  $\text{LiTa}_2\text{PO}_8$  hybrid-solid electrolyte (LTPO-HSE) is equal to  $-785/-594 \text{ J g}^{-1}$  (Table 1), while the glass fiber-

liquid electrolyte (GF-LE) is  $-1973/-1790 \text{ J g}^{-1}$ . It means that the cells assembled with LTPO-HSE produce less heat and will exhibit lower temperature [37].

Table 1. Comparison of LTPO-HSE, GF-LE QSSEs [37].

Parameters	LTPO-HSE	GF-LE
Li <sup>+</sup> - transference number	0.78	0.35
Average Li <sup>+</sup> diffusion coefficient( $\text{cm}^2 \text{ s}^{-1}$ )	$1.06 \times 10^{-10}$	$8.68 \times 10^{-12}$
Onset potential(V vs. Li/Li <sup>+</sup> )	5.25	3.5
Li-anode stability( $1 \text{ mA cm}^{-2}$ , $1 \text{ mAh cm}^{-2}$ )	Uniform Li plating/stipping	Non-uniform Li plating/stipping
Cycling stability( $0.5\text{C}/0.5\text{C}-350\text{cyc}$ )	81%	64%
Rate capability(capacity at 10C, $\text{mAh g}^{-1}$ )	370	270
Charge-transfer resistance(EIS, $\Omega$ )	46.7	74.6
Heat-generation( $5\text{C}$ , $\text{J g}^{-1}$ )	$-785/-594(\text{DC/CC})$	$-1937/-1790 (\text{DC/CC})$

In another study, a breakthrough improvement of QSSE for LSBs was obtained by dissolving lithium lanthanum tantalum zirconate (LLZTO) and polyethylene oxide in acetone [38]. The obtained solution coated on the conventional separator and dried at  $60^\circ\text{C}$ . After cooling, the polymer film soaked in commercial LE for 2 min. The produced electrolyte has shown  $0.8 \times 10^{-3} \text{ S cm}^{-1}$ .

The novel sodium super ionic conductor (NASICON-type) lithium aluminium germanium phosphate (LAGP) composite additive composed of  $\text{Li}_2\text{CO}_3$ ,  $\text{Al}_2\text{O}_3$ ,  $\text{GeO}_2$ , and  $\text{NH}_4\text{H}_2\text{PO}_4$  is used in the study by Wei et al [39]. LAGP containing electrolyte prepared by solution casting technique by mixing polyvinylidene fluoride (PVDF), LiTFSI and LAGP in the solvent n-methylpyrrolidone. Obtained liquid poured into a mold made of polytetrafluoroethylene. The mix of 1-butyl-1-methyl pyrrolidine bis-trifluoromethanesulfonimide ( $\text{Py}_{14}\text{TFSI}$ ) and LiTFSI used as LE. Improved mechanical characteristics, decreased interfacial resistance, suppressed dendritic formation, improved thermal and electrochemical stability, and improved lithium-ion transport are all attributed to LLZTO. As an inorganic filler, it preserves structural integrity, lowers resistance at the electrolyte-electrode interface, and offers a high-conductivity route for effective charge/discharge cycles [39].

The article by Shanet al discusses the development of a LiTFSI/ $\text{Py}_{14}\text{TFSI}$ / cellulose acetate (CA)/PVDF PE with strong ionic conductivity ( $1.45 \times 10^{-4} \text{ S cm}^{-1}$ ) and a large electrochemical stability window ( $4.95 \text{ V}$ ) [40]. Figure 7 depicts the impact of each addition, as well as the

relationship between ionic conductivity and tensile strength. This solid-state electrolyte effectively reduces the challenges associated with lithium-ion transport across the electrode's solid-solid interface and the electrolyte.

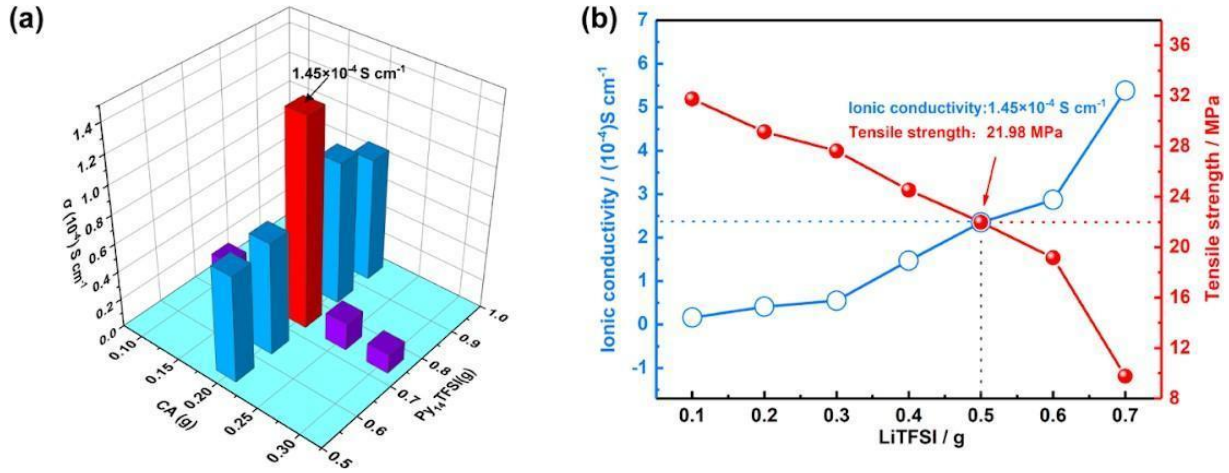


Figure 7. (a) Impact of various additives on the conductivity of LiTFSI/Py<sub>14</sub>TFSI/CA/PVDF electrolytes; (b) dependence of ionic conductivity on LiTFSI weight and tensile strength of LiTFSI/Py<sub>14</sub>TFSI/CA/PVDF electrolytes [40].

Improved lithium-ion transference number and lower interfacial impedance supplied by Py<sub>14</sub>TFSI. Adding Py<sub>14</sub>TFSI to the electrolyte increased the Li<sup>+</sup> transference number from 0.120 to 0.231 while decreasing interfacial impedance, as evidenced by a decrease in polarization voltage from 0.08 to 0.04 V. These modifications upgrade the overall performance and cycling stability of the ASSLSB. These findings directly address key challenges in ASSLSB development, such as boosting ionic conductivity, lowering interfacial impedance, and improving electrode compatibility with the solid-state electrolyte. The investigation of high-performance QSSEs and the escalation of the electrode-electrolyte interface are essential steps toward commercial viability for ASSLSBs. The study focuses on a specific PE composition (LiTFSI/Py<sub>14</sub>TFSI/CA/PVDF) and does not compare the performance of other formulations. Research on the use of lithium lanthanum zirconium oxide (LLZO) as an additive in QSSEs for LSBs has shown promising results in enhancing ionic conductivity and overall battery performance. According to a study, combining LLZO with an ionic LE greatly increased the ionic conductivity. The immaculate LLZO ceramic powder's ionic conductivity was measured at  $10^{-6} \text{ S cm}^{-1}$ ; at ambient temperature, the conductivity of the composite electrolyte, which consisted of LLZO mixed with ionic liquids, was  $10^{-3} \text{ S cm}^{-1}$ . Better lithium-ion conduction and overall battery efficiency are made possible by this improvement.

Moreover, the studies revealed that applying LLZO as an additive in QSSE increases not only the ionic conductivity but also has a positive effect on overall electrolyte structure, assisting in the long life of the battery [10].

In another study, the ionic-liquid-assisted  $\text{Py}_{14}\text{TFSI}$  compound was incorporated into the solution of PVDF and LiTFSI (Figure 8). Ionic liquid, which plays a role of LE, was added during the assembly of cells [37]. A magnificent conductivity higher than  $7.2 \times 10^{-4} \text{ S cm}^{-1}$  was reached.

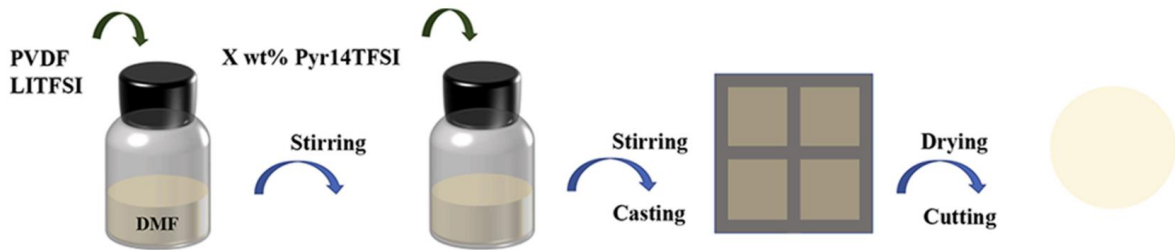


Figure 8. Visual presentation of producing PE by solvent casting method [41].

The article by Lee et al obtained a composite PE using PVDF-HFP and LLZTO highlighting the effect of electrospun fiber diameter on ionic conductivity [42]. Firstly, LLZTO and polyvinylpyrrolidone (PVP) were electrospun at 20 kV with PVP ratio varying between 8-12 wt%. Then obtained fibers were calcined  $750^{\circ}\text{C}$  for 2.5 h resulting in 80-290 mean diameter nm. Subsequently the mixture consisting of PVDF-HFP, LiTFSI casted onto the LLZTO/PVP fiber. According to the Nyquist plot shown in Figure 9, the ionic conductivities of composite solid electrolyte (CSE) in this study  $7.4 \times 10^{-5} \text{ S cm}^{-1}$ ,  $1.2 \times 10^{-4} \text{ S cm}^{-1}$ ,  $1.7 \times 10^{-4} \text{ S cm}^{-1}$ ,  $3.8 \times 10^{-4} \text{ S cm}^{-1}$  for 6  $\mu\text{m}$ , 290 nm, 140 nm, 80 nm samples respectively.

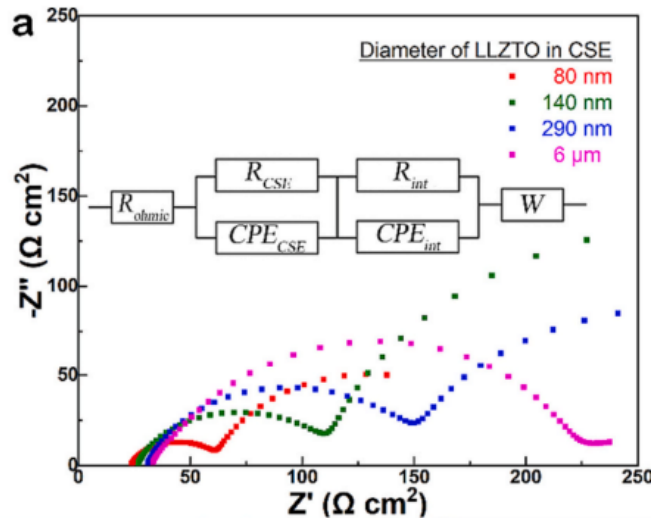


Figure 9. Nyquist plot of influence of LLZTO diameter on resistance of CSE [42].

The study by Du et al PVDF-HFP, LiTFSI, succinonitrile were mixed in ratio 6:4:2.5 and the 6-18% LLZTO was introduced to the system [25]. The solid PE was stirred with LiFePO<sub>4</sub> (LFP) cathode and acetylene black carbon additive. The best performance of ionic conductivity was shown by the sample containing 9.1 wt% LLZTO. The battery was assembled using LFP cathode and Li metal anode (LMA) without any LE (Figure 10).

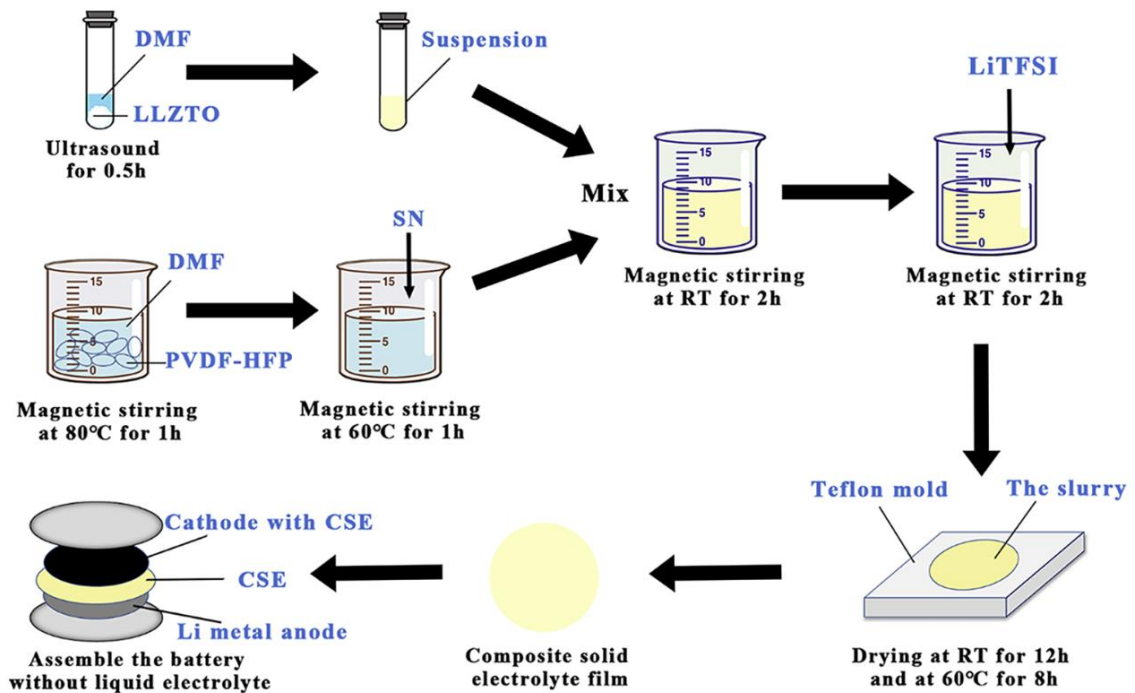


Figure 10. Visual representation of PVDF-HFP/ LiTFSI/LLZTO electrolyte processing [25].

In the next study reported by Gu et al, the ratio of PVDF-HFP:LiTFSI remains the same as previously reported work 6:4, while the content of LLZTO varies from 0-20% [43]. Both electrode materials were casted on foil, then the electrolyte layer was casted onto the electrodes. Then two electrodes were cold pressed to assemble the cell without any LE. The highest values of ionic conductivity ( $10^{-3} \text{ S cm}^{-1}$ ) and widest potential window (5.5V) are presented by 15% LLZTO sample. The CE of LIBs assembled using the 15% LLZTO sample were 84% and the capacity retention rate 94% within the first 30 cycles. The work gives insight into the potential of garnet-based electrolytes in LIBs and provides information about the optimal concentration of LLZTO.

The article by Cai et al investigates the influence of adding Ga into the ionic conductivity of PE and compares to Ga-LLZO preparation techniques regarding ion conduction of PE [44]. The ceramic-polymer composite electrolyte consisting of PVDF-HFP, LiTFSI with weight ratio 2:1, and 10% Ga-LLZO content. All solid components were dissolved in DMF, casted and dried at  $80^{\circ}\text{C}$  for 3 h. Their findings demonstrate that adding Ga-LLZO prepared via electrospinning outperform samples prepared by sol-gel method in terms of ionic conductivity ( $1.1 \times 10^{-4} \text{ S cm}^{-1}$ )  $\text{Li}^{+}$  transference number (0.87) and stability (700 cycles with 96.5% capacity retention).

To conclude the simplicity of process, uniform thickness of material makes the solution casting the most widely used solid electrolyte creating technique. Also, a great number of research completed via solution casting makes the technique favorable.

### 2.3.3 Phase inversion

Phase inversion (Figure 11) is a method where the homogeneous solution of a polymer transforms into a solid state by removing the solvent [45].

By presenting a unique double-layer hybrid solid electrolyte (DLHSE), the study by Liu et al makes a substantial contribution to the area of LSBs [3]. The novel arrangement tackles important issues in solid-state batteries, including the shuttle effect, emerging of dendrites, and interphase instability. A garnet-type LLZO layer and a NASICON-type lithium lanthanum titanate phosphate (LATP) layer make up the DLHSE. This mixture inhibits the production of dendrites and guarantees strong lithium-ion conductivity. By creating a three-dimensional network, a polymer binder poly(vinylidene fluoride-trifluoroethylene) improves the composite electrolyte's structural stability. The DLHSE outperforms several solid-state electrolytes now on the market with an ionic conductivity of  $1.03 \times 10^{-3} \text{ S cm}^{-1}$  at  $30^{\circ}\text{C}$ . After 500 cycles at 0.2C, the battery system maintains an impressive  $802 \text{ mAh g}^{-1}$  of capacity with no capacity decline. At the cathode contact, LATP enhances lithium-ion migration and reaction kinetics. LLZO improves the stability of the LMA contact and effectively inhibits the formation of dendrites. The work demonstrates the DLHSE's

potential for practical uses by verifying its viability in a prototype 7 Ah pouch cell. The combination of LEs, polymer binders, and inorganic ceramic layers produces a well-balanced electrolyte system with superior mechanical stability and good conductivity.

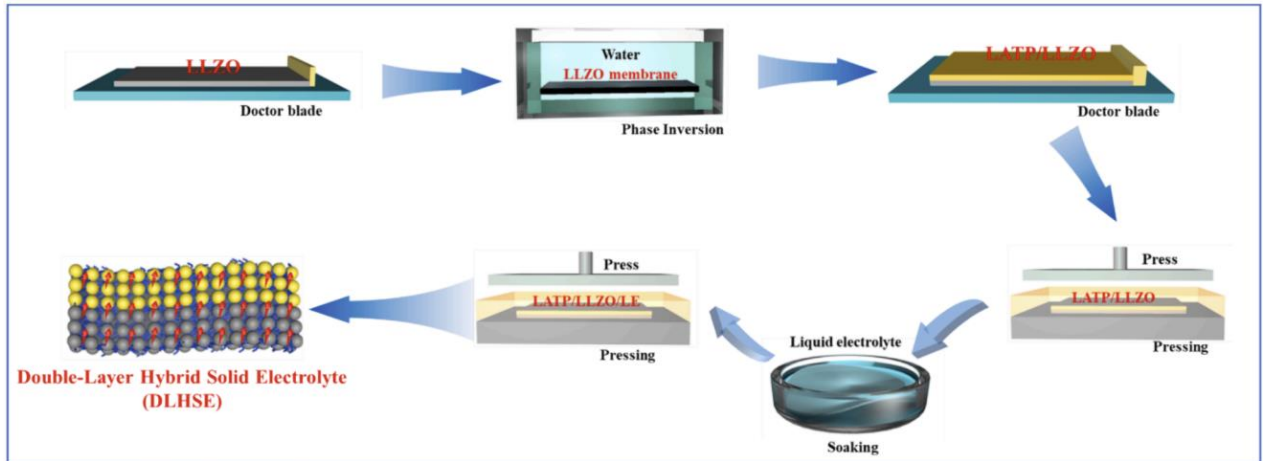


Figure 11. Visual representation of DLHSE fabrication [3].

Comprehensive insights into the Li-ion conduction routes and interfacial characteristics are provided by detailed characterization methods, such as Magic-Angle Spinning Nuclear Magnetic Resonance Spectroscopy and SEM. The methodical strategy for improving lithium-ion transport and inhibiting the polysulfide shuttle effect establishes a standard for further study in LSBs.

Although the DLHSE exhibits great ionic conductivity and continuing stability, it is yet unknown how scalable and economical this technology will be for large-scale manufacturing. More research is necessary to identify DLHSE's long-term stability under various operating and temperature settings. The study enhances the practical use of solid-state LSBs by contributing a novel electrolyte design. Through the integration of novel materials and arrangements, the DLHSE tackles long-standing issues in the sector and lays the groundwork for further developments.

In conclusion, high mechanical stability and good interface contact can be provided via phase inversion, but the selectivity to the composition of electrolyte, complexity of process and limited number of research completed via phase inversion cease the wide application of method.

### 2.3.4 Electrospinning

Electrospinning is the method of obtaining fibers and particles from polymer solution using voltage; the electrospinning process is ruled by an electro-hydrodynamic phenomenon [46].

Electrospinning technique starts with obtaining a solution of polymer. Polymer should be

uniformly distributed within the solvent molecules, also the solution should have appropriate viscosity, concentration, and electric conductance. The process parameters such as distance, voltage, feed rate and spinneret diameter can be changed depending on the features of the sample. The solution comes from the nozzle of the syringe and due to the high voltage becomes solid fiber.

The creation of a covalent organic framework (COF) electrolyte functionalized with sulfhydryl for QSSLBs is examined in a study completed by Bi et al [47]. It tackles important issues with battery performance, specifically minimizing the shuttle effect brought on by soluble lithium polysulfides and reaching an ideal electrolyte to sulfur ratio (E/S ratio). By combining sulfhydryl and imine-functionalized COFs (COF-SH) with PVDF-HFP fibers, the novel COF-SH@PVDF-HFP electrolyte produces robust polysulfide adsorption and catalytic conversion along with improved lithium-ion conductivity.

A wide range of sophisticated characterization techniques are used in the study, such as density functional theory simulations, FTIR, Raman spectroscopy, ultraviolet-visible spectroscopy, and X-ray photoelectron spectroscopy. These methods confirm that the COF-SH electrolyte has a strong chemical bond with polysulfides and can efficiently catalyze their conversion. The shuttle effect is suppressed and redox reactions are accelerated by this functionalized COF design, which improves cycling efficiency and capacity retention.

The experimental findings show that the COF-SH@PVDF-HFP-based LSBs exhibit remarkable electrochemical performance. With a capacity fading rate of only 0.03% per cycle, it maintains 77.3% of its initial capacity of 808.4 mAh g<sup>-1</sup> at a rate of 2C after 800 cycles. In comparison to traditional PVDF-HFP membranes, the study also reveals a greater lithium-ion migration number (0.52) and improved ionic conductivity ( $3.3 \times 10^{-3}$  S cm<sup>-1</sup>). Additionally, even at low E/S ratios and high current densities, the QSSE shows excellent rate performance and long-term lifecycle.

The article by Shanti et al demonstrated a novel composite electrolyte using PVDF-HFP, LiTFSI and various types of SiO<sub>2</sub>, and TiO<sub>2</sub> as a ceramic additive [48]. The composite electrolyte is prepared by dissolving PVDF-HFP (10%) and LiTFSI (0.1%) in the mixture of DMF/acetone (7/3, w.w) for 12 h in 50°C. Then the polymer solution was stirred with ceramic additive (0.1%). The electrospinning parameters were 1 ml h<sup>-1</sup>, 20 kV, 15 cm distance between the syringe and collector. Electrospun fibers were dehumidified using a vacuum oven at 60°C within 12 h. Obtained fibers were activated by immersing into LE which consists of DOL/Dimethyl ether (1/1, vol%) with 1.8 M LiTFSI and 1 M LiNO<sub>3</sub>. The highest ionic conductivity was displayed by the sample composed using nm-SiO<sub>2</sub>. Figure 12a displayed the SEM images of a polymer matrix composed of only PVDF-HFP and LiTFSI.

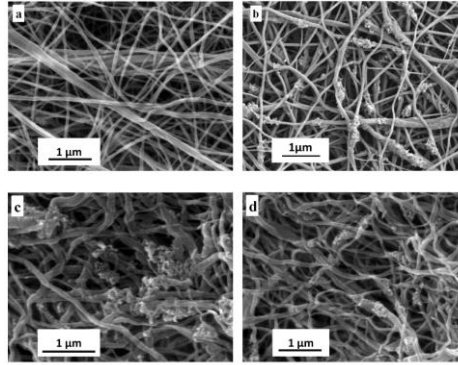


Figure 12. SEM images of (a) PVDF-HFP, LiTFSI prepared via electrospinning, (b) PVDF-HFP, LiTFSI, f-SiO<sub>2</sub> prepared via electrospinning, (c) PVDF-HFP, LiTFSI, nm-SiO<sub>2</sub> prepared via electrospinning, and (d) PVDF-HFP, LiTFSI, nm-TiO<sub>2</sub> prepared via electrospinning [48].

In another study by Nikodimos et al a GPE has been prepared utilizing PVDF-HFP and LAGP ceramic additive [49]. The solution PVDF-HFP including 0, 5, 10, 15, 20% LAGP prepared by dissolving DMF for 12 h. Electrospinning parameters were 14.3 kV and 15 cm distance from needle till collector. Additional innovation of this article were assembling batteries without peeling the electrospun fibers from Cu foil current collector. The Figure 13 shows the difference in ionic conductivity of the unpeeled polymer film with Cu indicated Cu@GPE|NMC and peeled polymer film indicated as Cu|cGPE|NMC.

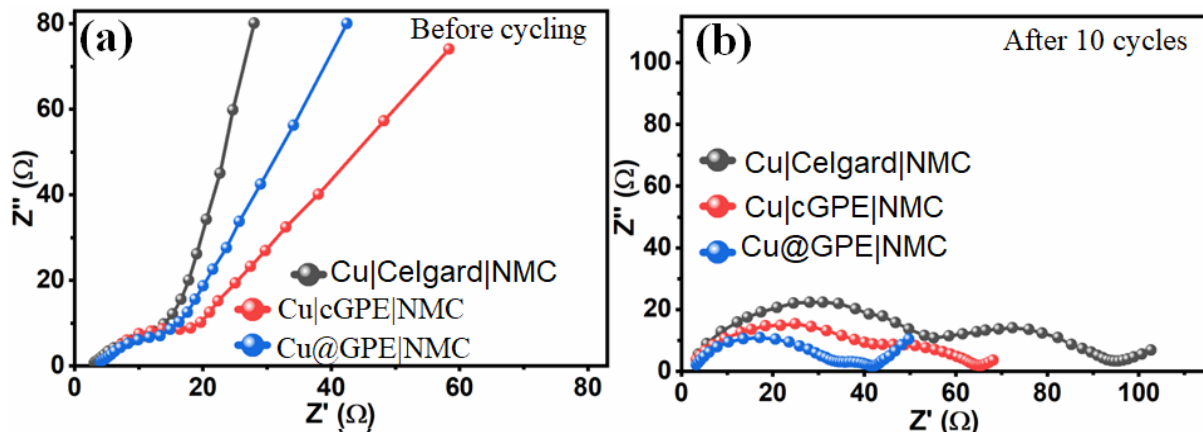


Figure 13. Nyquist plots of the GPE (a) before cycling and (b) after 10 cycles [49].

Electrospinning is one of the popular methods of producing PE, despite the drawbacks like time consumption, high cost, low production capacity and low mechanical strength of products.

Mechanical properties of products are being improved via ceramic additives and plasticizers. Moreover, researchers found out that electrospinning outperforms sol-gel technique [44], thus the electrospinning can be considered beneficial regarding ion conduction.

This study focus on LiTFSI and PVDF-HFP-based QSSE for LSBs. Enhancing ionic conductivity while inhibiting the polysulfide shuttle effect which seriously impairs the functionality and durability of LSBs is the main goal.

To create the PEs, three manufacturing methods were methodically used: electrospinning, solution casting, and spin coating. According to a comparative examination, the electrospinning process performed better than the others, as evidenced by better ionic conductivity, increased amorphous properties, improved polymer-salt interactions, and improved salt dispersion. Effective ion conduction was made possible by the continuous routes for lithium-ion transport that the porous and nanofibrous structure produced by electrospinning offered.

All things considered, the study shows that creating high-performance QSSEs requires careful consideration of both the right production techniques and the best possible material composition. The results offer important new information for developing QSSE technology for safer and more useful lithium-sulfur battery applications.

Despite extensive research into the development of QSSEs for LSBs, there is still a lack of systematic comparative studies evaluating the influence of different fabrication techniques on the structural, morphological, and electrochemical properties of QSSEs based on the same material composition. Most present research focuses on specific production processes rather than directly evaluating their efficacy in improving salt dispersion, lowering crystallinity, and increasing ionic conductivity. Furthermore, striking the right balance between ionic conductivity and mechanical stability remains a significant issue, especially for electrospun membranes, which frequently have low mechanical strength despite their greater ionic conductivity. Furthermore, minimal research has been conducted to determine the scalability, homogeneity, and practical usability of electrospinning, solution casting, and spin coating processes for large-scale battery manufacture.

The electrospinning technique was selected for its exceptional ability to produce highly porous, interconnected nanofibrous membranes. By offering constant ion movement paths, this shape improves the QSSE's ionic conductivity. Additionally, by increasing the amorphous content and promoting greater salt dispersion within the polymer matrix, electrospinning lowers crystallinity and improves ion transport. High-performance QSSEs depend on improved ionic conductivity, which electrospinning provides a clear advantage in achieving despite significant drawbacks including low mechanical strength and restricted scalability.

Solution casting was used because technique is simple, inexpensive, and can make membranes of uniform thickness. This approach is commonly used in laboratory-scale QSSE

manufacturing to provide a baseline for performance comparison. However, solution-cast membranes have a greater crystallinity, which may impede ionic mobility. Nonetheless, its simplicity of processing and repeatability make it an indispensable approach for preliminary material assessment.

Spin coating was chosen because of its capacity to create ultrathin electrolyte layers with better electrode-electrolyte interfacial contact. This approach enables for exact control of film thickness, which can greatly reduce interfacial resistance in battery systems. While spin coating can often result in non-uniform thickness across vast regions, its ability to generate thin, compact layers makes it an appropriate approach for QSSE manufacturing, particularly for enhancing interfacial characteristics. Benefits and drawbacks of each PE obtaining method is summarized in Table 2.

Table 2. The benefits and drawbacks of QSSE fabrication methods

Method	Benefits	Drawbacks	Sources
In-situ polymerization	Enhanced interfacial contact, stability of structure	Lengthy process, complex reactions, unpolymerized monomers can stay in cell	[50]
Solution casting	Simplicity of process, uniform thickness of product	Limited mechanical strength	[37]
Phase inversion	Tailored porosity, high mechanical stability	Complexity of process, not all type of polymer can be composed using this technique	[45]
Electrospinning	Highly porous product, nanosize fibers can be obtained	Time-consuming process, high cost, low production capacity, limited mechanical strength	[46]
Spin coating	Minimal thickness of electrolyte, improved interfacial contact between electrode and electrolyte	Time consuming process, nonuniform thickness of film	[51]

# Chapter 3 - Experimental section

## 3.1 Materials

The PVDF-HFP with an average molecular mass of ~400 000, DMF (99.8%), acetone (99.8%), LiTFSI ( $\geq 99.0\%$ ) were purchased from Sigma-Aldrich (Merck). All the purchased chemical reagents were analytical grade and used without any purification.

## 3.2 Preparation of PE

The PE with PVDF-HFP and various concentrations of LiTFSI (0-16 wt.%) was prepared using the following procedure. A solvent combination consisting of acetone and DMF at a weight ratio of 7:3 was used to dissolve 16 wt.% PVDF-HFP. Once PVDF-HFP was entirely dissolved, LiTFSI was put into the solution. The resulting mixture was stirred overnight at 50°C and 330 rpm to ensure thorough dissolution and uniform distribution of LiTFSI within the polymer matrix.

### 3.2.1 Electrospinning technique

The solution, after being stirred overnight, was transferred into a 20 mL plastic syringe and placed in the electrospinning apparatus for injection. Drum collector was covered with ultra-high vacuum Al foil to obtain fibers. The electrospinning parameters applied to obtain polymer fibers were: 1.3 ml h<sup>-1</sup> flow rate, distance between nozzle and collecting foil 15 cm and voltage 30 kV. Also, the drum was moving horizontally for 30 mm, with speed 10mm s<sup>-1</sup>. The drum rotation speed 100 rpm. After the fibers were obtained, the solvent was removed by drying Al foil with electrospun polymer for 12 hours at 60°C.

### 3.2.2 Solution casting technique

Overnight stirred solution were spread onto Al foil using a doctor blade. The thickness of the doctor blade was 20  $\mu\text{m}$ . After slowly and uniformly applying solution, Al foil with polymer film was dried for 12 h at 60°C to remove the excess solvent.

### 3.2.3 Spin coating technique

Solution were spin coated for 45 s, rotation speed 7000 rpm and acceleration 2000 rpm. This procedure was repeated 4 times, obtained polymer films heat treated for 12 h at 60 °C.

### 3.3 Physical characterizations

The physical properties of 3 samples and components of PE: PVDF-HFP and LiTFSI were investigated using SEM-EDS, XRD and FTIR. The XRD and FTIR analysis were conducted without any modification. For taking SEM image samples were first coated with a conducting metal layer with 5  $\mu\text{m}$ .

### 3.4 PEIS analysis

First, to conduct the PEIS analysis between two stainless steel coin cell parts were washed using ethanol and fully dried. The coin cell 2032 part construction is displayed in Figure 14.

The PEIS analysis was carried out utilizing the Autolab instrument in frequency range between  $10^5$  Hz and 0.1 Hz starting from room temperature till  $60^\circ\text{C}$  to investigate the effect of temperature on ionic conductivity.

The ionic conductivities of PE were calculated using the following equation:

$$\sigma = l / R * A$$

where:

$\sigma$  - ionic conductivity,

$l$  - thickness of PE,

$R$  - resistance,

$A$  - area.



Figure 14. Schematic representation of coin cell assembling for PEIS analysis.

## Chapter 4 - Results and discussion

### 4.1 Effect of LITFSI concentration on the physical properties of QSSE prepared by electrospinning

One of the ways of improving the ionic conductivity of PE is increasing the concentration of lithium salt added to the polymer. On the other hand, addition of the salt and increasing its concentration in the electrospinning solution can significantly affect the fiber formation, morphology and properties of the resultant fibers. In this regard, finding an optimal concentration of the salt that provides balance between the ionic conductivity and other physical properties of the fibers is important.

Figure 15 illustrates SEM images of PVDF-HFP-based PE with/out LITFSI of different concentrations, where formation of the fibers can be confirmed for all concentrations. On the other hand, significant differences in the morphology depending on concentration is observed. Thus, the fibers made of lower LITFSI concentrations ( $\leq 5\%$ ) form polymer networks with uniformly distributed voids and hollows (Figure 15 (a-d), while fibers made of higher LITFSI concentrations ( $>5\%$ ) tend to adhere to each other, causing non-uniform distribution of fiber diameter (Figure 15(e-g)).

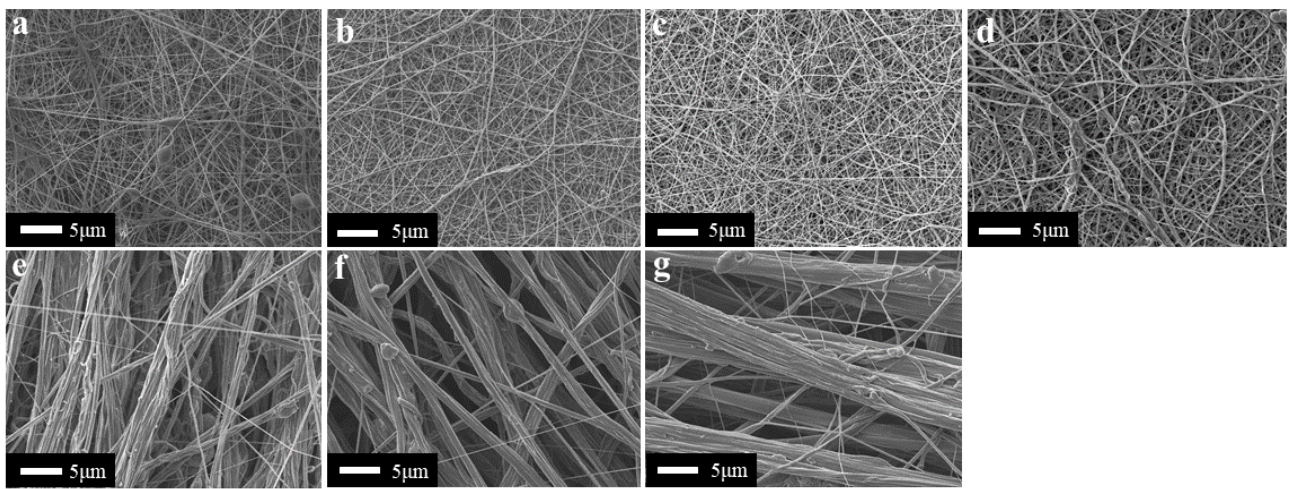


Figure 15. SEM images of samples prepared via electrospinning with (a) 0%, (b) 1%, (c) 3%, (d) 5%, (e) 7%, (f) 10%, and (g) 16% LiTFSI.

To investigate the accurate thickness of PVDF-HFP-based PE with LITFSI of different concentrations, the cross-sectional SEM was conducted and displayed in Figure 16.

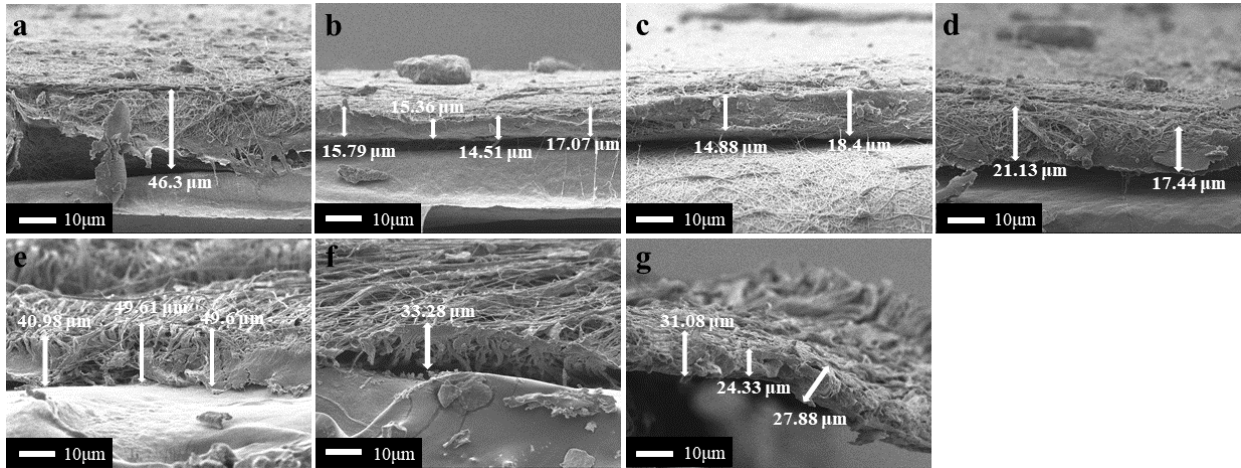


Figure 16. Cross-sectional SEM images of samples prepared via electrospinning with (a) 0%, (b) 1%, (c) 3%, (d) 5%, (e) 7%, (f) 10%, and (g) 16% LiTFSI.

To examine the ionic conductivity of samples, PEIS analysis was conducted. Nyquist plots of PVDF-HFP-based PE with LITFSI of different concentrations are shown in Figure 17. The resistance of PE is identified by the intersection of lines with the real (Ox) axis. Figures 17(a), 17(b), and 17(d), corresponding to 0%, 1%, and 5% LiTFSI, respectively, exhibit the expected Nyquist plot characteristics, including the semicircular arc and Warburg impedance. In contrast, Figure 17(c) only displays a partial semicircle. Nyquist plots of 7-16% LiTFSI samples display different characteristics without any cemicircle and Warburg plot as in Figure 17(a). Moreover, increasing the temperature escalates the difference between 17(a) and 17(e,g). Thus, the high-temperature results of PEIS analysis of 7%, 16% LiTFSI samples were not included in 17(e, g).

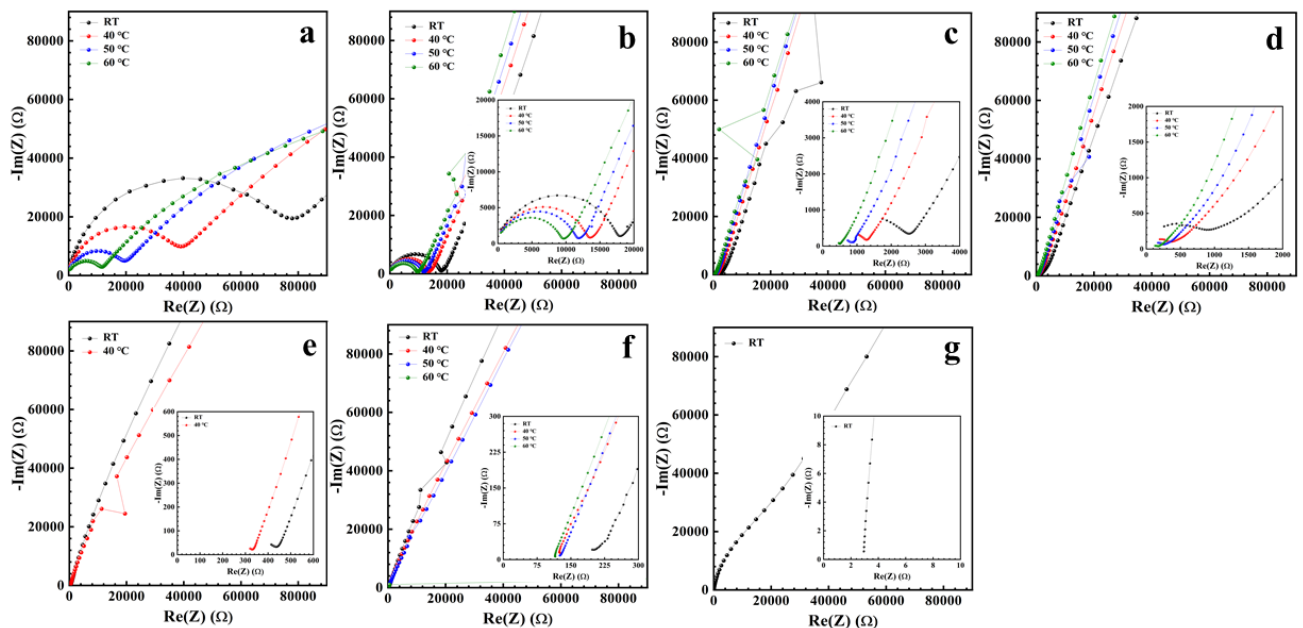


Figure 17. Nyquist plot of samples (a) 0%, (b) 1%, (c) 3%, (d) 5%, (e) 7%, (f) 10%, and (g) 16% LiTFSI prepared via electrospinning.

According to Figure 17 and Table 3, the increasing concentration of LiTFSI enhances ionic conductivity. However, due to fiber agglomerating (Figure 15) and Nyquist plot changes, the 5% LiTFSI sample is considered reliable.

Table 3. Ionic conductivity of PE obtained via electrospinning.

$\sigma$ , $10^{-6}$ S $\text{cm}^{-1}$	RT	40 °C	50 °C	60 °C
0% LiTFSI	0.01	0.02	0.04	0.06
1% LiTFSI	0.04	0.06	0.07	0.08
3% LiTFSI	0.26	0.51	0.81	1.29
5% LiTFSI	1.11	2.50	3.33	5.55
7% LiTFSI	3.62	4.83	x	x
10% LiTFSI	5.86	9.01	9.37	10.19
16% LiTFSI	325.58	x	x	x

#### 4.2 Effect of preparation method on the physical properties of QSSE

The sample with the highest value of ionic conductivity obtained via electrospinning were also prepared via spin coating and solution casting. This part of the study focuses on the dependence of ionic conductivity, morphology, crystallinity, and thermal stability on preparation techniques.

XRD analysis was used to investigate the crystallinity and possible phase separation in PVDF-HFP/LiTFSI PE films made by solution casting, electrospinning, and spin coating. Figure 18 shows XRD patterns of pure LiTFSI, PVDF-HFP, and composite films made using each technique, spanning a  $2\theta$  range of  $10^\circ$  to  $90^\circ$ . Pure LiTFSI has crisp, well-defined peaks suggesting strong crystallinity, while PVDF-HFP shows wide peaks  $18.81^\circ$ ,  $20.43^\circ$ ,  $26.84^\circ$ ,  $39.22^\circ$  indicating its semi-crystalline  $\alpha$ -phase. With the addition of LiTFSI the peaks at  $26.84^\circ$ ,  $39.22^\circ$  almost disappear which indicates the decrease of crystallinity of PVDF-HFP [52].

Among the polymer films, electrospun sample preserves distinct LiTFSI peaks and minor characteristics like PVDF-HFP reflections, indicating high crystallinity of sample. The solution casted film likewise has both PVDF-HFP and LiTFSI peaks, implying partial salt recrystallization.

In contrast, the spin coated film has a broad, diffuse profile with no obvious LiTFSI peaks, indicating a primarily amorphous structure. Overall, these findings suggest that solution casting and spin coating result in more homogenous salt dispersion and lower crystallinity than solution casting.

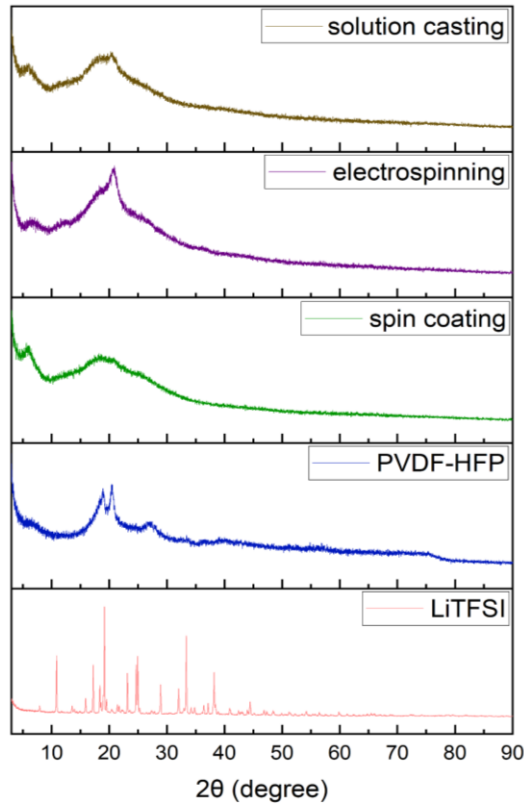


Figure 18. XRD analysis of 5% LiTFSI sample prepared by electrospinning, solution casting, and spin coating.

To investigate the chemical composition and ion-polymer interaction and main functional groups FTIR analysis was carried out. Figure 19 depicts the FTIR spectra of pure PVDF-HFP, LiTFSI and polymer films obtained via spin coating, electrospinning and solution casting. The PVDF-HFP shows peaks corresponding to  $\alpha$  phase of polymer  $762\text{ cm}^{-1}$  (C-F<sub>2</sub> bending),  $796\text{ cm}^{-1}$  (C-F<sub>3</sub> stretching),  $974\text{ cm}^{-1}$  (out-of-plane C-H bending or twisting) [53]. Also, peaks observed at  $872\text{ cm}^{-1}$  (C-H<sub>2</sub> wagging in vinylidene groups, amorphous HFP),  $1058\text{ cm}^{-1}$  (symmetric C-F<sub>3</sub> stretching, amorphous HFP),  $1178\text{ cm}^{-1}$  (asymmetric C-F stretching),  $1383\text{ cm}^{-1}$  (C-H<sub>2</sub> wagging vibration), and  $1404\text{ cm}^{-1}$  (C-H<sub>2</sub> scissoring vibration). The peak at  $1640\text{ cm}^{-1}$  represents the complexation of LiTFSI with PVDF-HFP [53]. According to FTIR spectra of LiTFSI peak at  $1061\text{ cm}^{-1}$  (C-F<sub>2</sub> symmetric stretching mode) is slightly shifted to  $1062\text{ cm}^{-1}$ ,  $1056\text{ cm}^{-1}$ ,  $1058\text{ cm}^{-1}$  respectively for electrospun, solution casted and spin coated samples. Shift to left implies the strong interaction with LiTFSI [54]. According to FTIR spectroscopy the solution casted sample has the highest amount of crystalline PVDF-HFP. Meanwhile the crystallinity degree of spin coated films was lower in comparison to electrospun fibers.

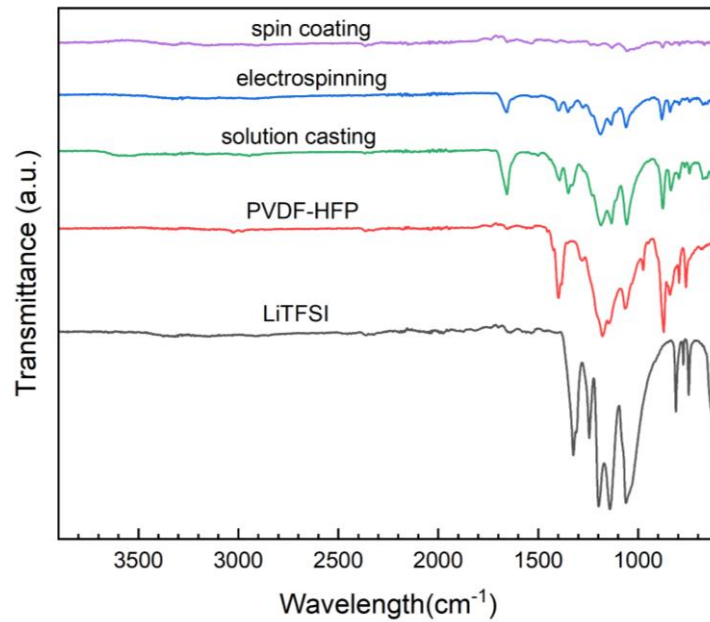


Figure 19. FTIR spectra of 5% LiTFSI sample prepared by electrospinning, solution casting, and spin coating.

The SEM-EDS analysis was completed to estimate the distribution of elements within the surface of samples. SEM-EDS results of 5% LiTFSI sample prepared via 3 methods are illustrated in Figure 20: (a) electrospinning, (b) solution casting, (c) spin coating. According to Figure 20 the sulfur intensity was much lower than other elements in all 3 samples. As the figures 20 b-c show, the samples prepared by solution casting, spin coating had voids in circular shape. The EDS of spin coated 5% LiTFSI demonstrates the exhibition of O, C in voids.

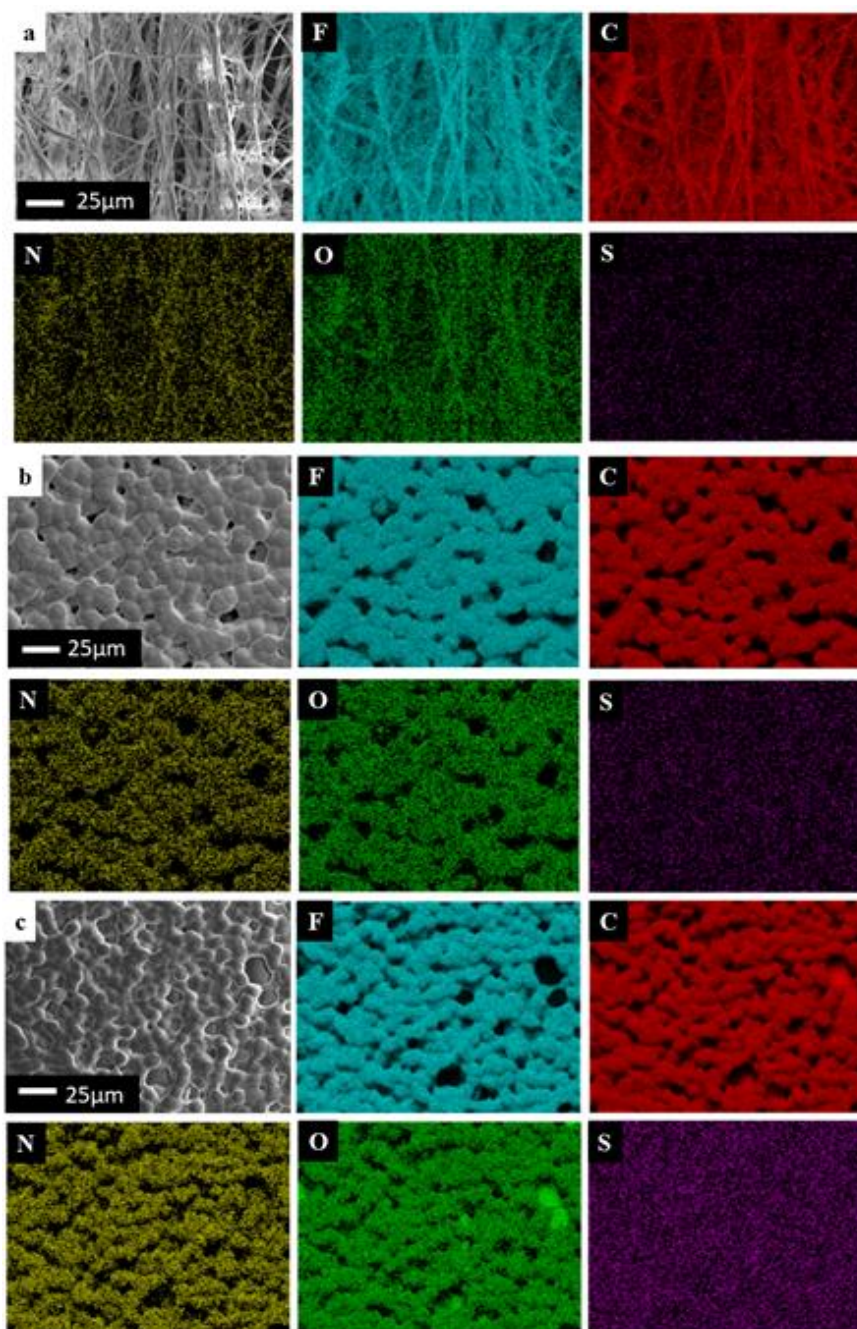


Figure 20. SEM-EDS characterization of 5% LiTFSI produced via (a) electrospinning, (b) solution casting, and (c) spin coating.

To investigate the thermal stability of PE heat treatment analysis was completed. Figure 21(a) displays the samples obtained via spin coating, electrospinning and solution (from left to right) casting before heat treatment. According to Figure 21(b) the thickness of spin coated sample reduced, the electrospinning sample shrunk and became hard plastic material, and the solution casted polymer film was the most resistant to heat.

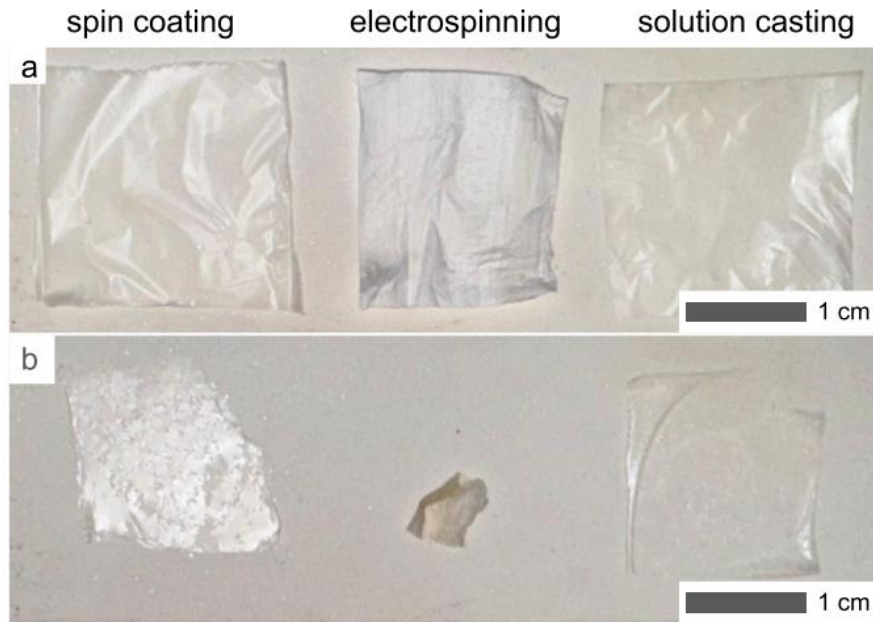


Figure 21. 5% LiTFSI samples (a) before and (b) after heat treatment.

The cross-section SEM images of 5% LiTFSI samples prepared via solution casting and spin coating were taken to identify the accurate thickness of electrolyte and illustrated in Figure 22.

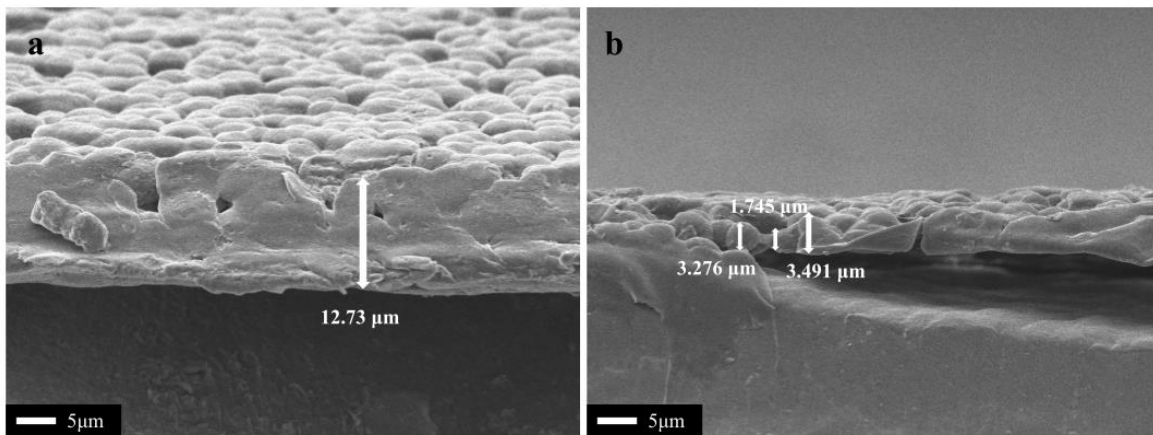


Figure 22. Cross-sectional SEM characterization of 5% LiTFSI produced via (a) solution casting, and (b) spin coating.

Nyquist plots of spin coated and solution casted PE, assembled under the same condition as mentioned above, are illustrated in Figure 23 (a, b). Figure 23a depicts the Nyquist plot of solution casted 5% LiTFSI sample with Warburg impedance. The results of spin coated 5% LiTFSI PEIS analysis provided in Figure 23b, as the figure shows the ordinary Nyquist plot was successfully obtained only at room temperature and 40 °C.

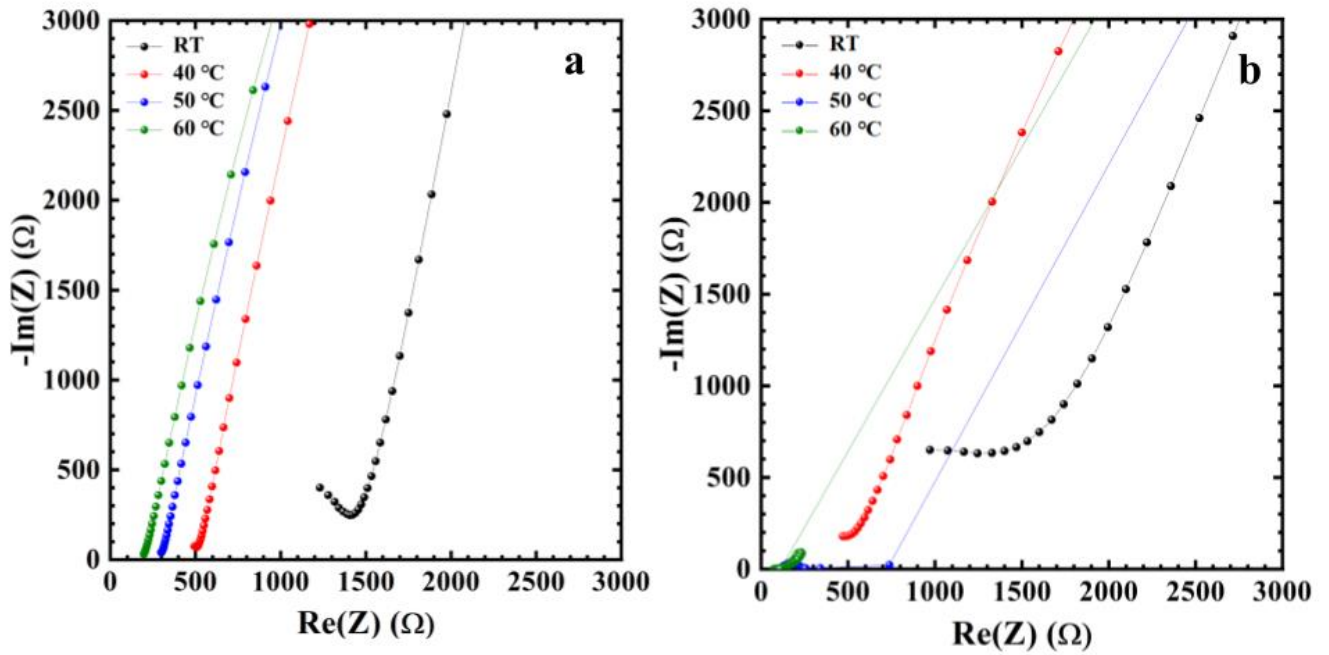


Figure 23. Nyquist plots of 5% LiTFSI prepared by (a) solution casting (b) spin coating.

Table 4 provides a combined outcome of Figure 23 and 24 with exact values of ionic conductivity. In comparison the ionic conductivity values of 5% LiTFSI obtained by electrospinning technique are 3.5 times and 15.8 times higher than solution casted, spin coated samples respectively.

Table 4. Ionic conductivity of 5% LiTFSI obtained via solution casting and spin coating approaches

$\sigma$ , $10^{-6}$ S $\text{cm}^{-1}$	RT	40 °C	50 °C	60 °C
solution casted 5% LiTFSI	0.32	0.89	1.49	2.24
spin coated 5% LiTFSI	0.07	0.19	x	x

To conclude, the optimal concentration of lithium salt added to PVDF-HFP/ LiTFSI is 5%, which is proved by PEIS and SEM. Increasing the LiTFSI content has detrimental effect on fiber formation. XRD and FTIR spectra patterns of 5% LiTFSI reveal that spin coating produces a largely amorphous structure with better salt distribution, favoring improved ionic transport. FTIR analysis reveals that electrospun membranes demonstrate more pronounced ion-polymer interactions and modest crystallinity. Also, investigation of various QSSE obtaining methods have shown that electrospinning has higher ionic conductivity.

### 4.3 Comparison with literature reported QSSEs

A quantitative comparison between the ionic conductivity values recorded in this work and those reported in recent literature for similar QSSEs was carried out to increase the contextual importance of the results obtained. At 60°C, the ionic conductivity of the electrospun PVDF-HFP/LiTFSI membrane with 5 wt. % LiTFSI was  $5.55 \times 10^{-6} \text{ S cm}^{-1}$ . Despite being small, this value was obtained without the use of ionic liquid additions or ceramic fillers, which are frequently utilized in previous experiments to increase conductivity. The in-situ polymerized QSSE based on IDCN was described by Judez et al. (2019) and has an ionic conductivity of about  $2.96 \times 10^{-4} \text{ S cm}^{-1}$  at ambient temperature. Similarly, Hu et al. (2018) used a gel polymer electrolyte consisting of SiO<sub>2</sub>, DOL, and SiCl<sub>4</sub> to produce a conductivity of  $5.37 \times 10^{-4} \text{ S cm}^{-1}$ . Wei et al. (2023) showed that a PVDF-based QSSE improved with LAGP ceramic filler and ionic liquid Py14TFSI had a conductivity of  $1.45 \times 10^{-4} \text{ S cm}^{-1}$ . Furthermore, an electrospun PVDF-HFP/LiTFSI membrane containing nano-SiO<sub>2</sub> was reported by Shanti et al. (2022) and achieved a high conductivity of  $3.3 \times 10^{-3} \text{ S cm}^{-1}$ . It is crucial to emphasize that the membrane made here contains only 5 wt. % LiTFSI and does not require any complicated additives or post-treatments, even if the conductivity attained in our study is lower than that of these cutting-edge systems. This highlights how well the polymer-to-salt ratio can be optimized and shows how electrospinning can be used as a scalable method to create functional polymer electrolytes. Future developments, including the addition of ceramic nanoparticles or plasticizers to further improve ionic conductivity and mechanical resilience, are strongly supported by improved polymer-salt interactions, consistent shape, and ease of production.

Table 5. Comparison of ionic conductivity values of various QSSE

Study	Composition	Method	$\sigma \text{ (S cm}^{-1}\text{)}$	Temperature (°C)
This work	PVDF-HFP + 5% LiTFSI	Electrospinning	$5.55 \times 10^{-6}$	60
[33]	IDCN + LiTFSI	In-situ polymerization	$2.96 \times 10^{-4}$	RT
[34]	SiO <sub>2</sub> + DOL + SiCl <sub>4</sub>	In-situ polymerization	$5.37 \times 10^{-4}$	RT
[39]	PVDF + LAGP + Py14TFSI	Solution casting	$1.45 \times 10^{-4}$	RT
[48]	PVDF-HFP + nano-SiO <sub>2</sub>	Electrospinning	$3.3 \times 10^{-3}$	RT

## Chapter 5 - Conclusions

In this study, polymer electrolytes (PEs) based on PVDF-HFP with varying concentrations of LiTFSI (0–16%) were synthesized via electrospinning. Initially, the LiTFSI content was optimized. SEM analysis of the resulting membranes revealed morphology changes depending on the salt content, providing insight into fiber structure and uniformity. Among the tested compositions, the sample with 5% LiTFSI exhibited the most favorable morphology and the highest ionic conductivity. Subsequently, the influence of different preparation methods electrospinning, solution casting, and spin coating on the physical and electrochemical properties was evaluated. All membranes were analyzed using SEM-EDS, FTIR, and XRD. XRD analysis revealed that the spin-coated sample had the lowest crystallinity, while FTIR results indicated stronger ion–polymer interactions in electrospun membranes compared to those produced by other methods. Overall, the electrospinning technique yielded membranes with superior ionic conductivity, making it the most effective fabrication method in this study. However, it should be noted that electrospun membranes exhibited lower thermal stability at elevated temperatures.

During completing this MSc Thesis, the author also contributed the article “Spin-coated Sulfur thin film cathode for Lithium-Sulfur microbattery” by A. Mashekova, A. Umirzakov, M. Yegamkulov, B. Uzakbaiuly, M. Aliyakbarova, A. Mukanova and Zh. Bakenov which were published in the Royal Society Chemistry journal.

# Bibliography

- [1] <https://tengizchevroil.com/tco-news/detail/2021/06/04/sulfur-granulation-plant-has-been-commissioned-at-tengiz>
- [2] X. Judez, M. Martinez-Ibañez, A. Santiago, M. Armand, H. Zhang, and C. Li, “Quasi-solid-state electrolytes for lithium sulfur batteries: Advances and perspectives,” *Journal of Power Sources*, vol. 438, p. 226985, Oct. 2019, doi: <https://doi.org/10.1016/j.jpowsour.2019.226985>.
- [3] Y. Liu, J. Han, D.-H. Baek, Hyun Woo Kim, J.-H. Ahn, and J.-K. Kim, “Unlocking high-energy solid-state lithium-sulfur batteries with an innovative double-layer hybrid solid electrolyte,” *Chemical Engineering Journal*, vol. 496, pp. 153647–153647, Jul. 2024, doi: <https://doi.org/10.1016/j.cej.2024.153647>
- [4] Milinda Kalutara Koralalage *et al.*, “Functionalization of Cathode–Electrolyte Interface with Ionic Liquids for High-Performance Quasi-Solid-State Lithium–Sulfur Batteries: A Low-Sulfur Loading Study,” *Batteries*, vol. 10, no. 5, pp. 155–155, Apr. 2024, doi: <https://doi.org/10.3390/batteries10050155>
- [5] D. Qiu *et al.*, “High-Performance Li-S Batteries with a Minimum Shuttle Effect: Disproportionation of Dissolved Polysulfide to Elemental Sulfur Catalyzed by a Bifunctional Carbon Host,” *ACS applied materials & interfaces*, vol. 15, no. 30, pp. 36250–36261, Jul. 2023, doi: <https://doi.org/10.1021/acsami.3c06459>
- [6] J. Chattopadhyay, Tara Sankar Pathak, and Diogo M.F. Santos, “Applications of Polymer Electrolytes in Lithium-Ion Batteries: A Review,” *Polymers*, vol. 15, no. 19, pp. 3907–3907, Sep. 2023, doi: <https://doi.org/10.3390/polym15193907>.
- [7] S.-H. Tian, J.-C. Wang, N. Zhang, P.-F. Wang, J. Zhang, and T.-F. Yi, “Key issues and modification strategies towards high-performance polymer all-solid-state lithium-sulfur batteries,” *Coordination Chemistry Reviews*, vol. 513, p. 215909, Aug. 2024, doi: <https://doi.org/10.1016/j.ccr.2024.215909>.
- [8] K. Siczek, “The Toxicity of Secondary Lithium-Sulfur Batteries Components,” *Batteries*, vol. 6, no. 3, p. 45, Sep. 2020, doi: <https://doi.org/10.3390/batteries6030045>.
- [9] S. Wang *et al.*, “Interfacial challenges for all-solid-state batteries based on sulfide solid electrolytes,” *Journal of Materiomics*, vol. 7, no. 2, pp. 209–218, Mar. 2021, doi: <https://doi.org/10.1016/j.jmat.2020.09.003>.
- [10] L. Mazzapioda, A. Tsurumaki, Graziano Di Donato, H. Adenusi, Maria Assunta Navarra, and S. Passerini, “Quasi-solid-state electrolytes - strategy towards stabilising Li|inorganic solid electrolyte interfaces in solid-state Li metal batteries,” *Energy materials*, Jan. 2023, doi: <https://doi.org/10.20517/energymater.2023.03>.

- [11] Yuhang. Shan, Libo. Li, and Xueying. Yang, “Solid-State Polymer Electrolyte Solves the Transfer of Lithium Ions between the Solid–Solid Interface of the Electrode and the Electrolyte in Lithium–Sulfur and Lithium-Ion Batteries,” *ACS Applied Energy Materials*, vol. 4, no. 5, pp. 5101–5112, Apr. 2021, doi: <https://doi.org/10.1021/acsaem.1c00658>
- [12] E. Umeshbabu, B. Zheng, and Y. Yang, “Recent Progress in All-Solid-State Lithium–Sulfur Batteries Using High Li-Ion Conductive Solid Electrolytes,” *Electrochemical Energy Reviews*, vol. 2, no. 2, pp. 199–230, Feb. 2019, doi: <https://doi.org/10.1007/s41918-019-00029-3>
- [13] T. Tao et al., “Understanding the role of interfaces in solid-state lithium-sulfur batteries,” *Energy materials*, vol. 2, no. 5, pp. 35–35, Jan. 2022, doi: <https://doi.org/10.20517/energymater.2022.46>
- [14] L.-P. Hou et al., “Improved interfacial electronic contacts powering high sulfur utilization in all-solid-state lithium–sulfur batteries,” *Energy Storage Materials*, vol. 25, pp. 436–442, Mar. 2020, doi: <https://doi.org/10.1016/j.ensm.2019.09.037>
- [15] C. Wang, J. Liang, Y. Zhao, M. Zheng, X. Li, and X. Sun, “All-solid-state lithium batteries enabled by sulfide electrolytes: from fundamental research to practical engineering design,” *Energy & Environmental Science*, vol. 14, no. 5, pp. 2577–2619, 2021, doi: <https://doi.org/10.1039/d1ee00551k>
- [16] R. K. Bhardwaj and D. Zitoun, “Recent Progress in Solid Electrolytes for All-Solid-State Metal(Li/Na)–Sulfur Batteries,” *Batteries*, vol. 9, no. 2, p. 110, Feb. 2023, doi: <https://doi.org/10.3390/batteries9020110>
- [17] S. Das, K. N. Gupta, A. Choi, and V. Pol, “Operando Fabricated Quasi-Solid-State Electrolyte Hinders Polysulfide Shuttles in an Advanced Li-S Battery,” *Batteries*, vol. 10, no. 10, p. 349, Oct. 2024, doi: <https://doi.org/10.3390/batteries10100349>.
- [18] É. A. Santos *et al.*, “Trends in ionic liquids and quasi-solid-state electrolytes for Li-S batteries: A review on recent progress and future perspectives,” *Chemical Engineering Journal*, vol. 493, p. 152429, May 2024, doi: <https://doi.org/10.1016/j.cej.2024.152429>.
- [19] Z. Xue, D. He, and X. Xie, “Poly(ethylene oxide)-based electrolytes for lithium-ion batteries,” *Journal of Materials Chemistry A*, vol. 3, no. 38, pp. 19218–19253, Sep. 2015, doi: <https://doi.org/10.1039/C5TA03471J>.
- [20] Z. M. Elimat, W. T. Hussain, and A. M. Zihlif, “PAN-based carbon fibers/PMMA composites: thermal, dielectric, and DC electrical properties,” *Journal of Materials Science Materials in Electronics*, vol. 23, no. 12, pp. 2117–2122, Apr. 2012, doi: <https://doi.org/10.1007/s10854-012-0712-y>.
- [21] Mukaddes Keskinates, B. Yilmaz, Yakup Ulusu, and Mevlut Bayrakci, “Electrospinning of novel calixarene-functionalized PAN and PMMA nanofibers: Comparison of fluorescent protein adsorption performance,” *Materials Chemistry and Physics*, vol. 205, pp. 522–529, Nov. 2017, doi: <https://doi.org/10.1016/j.matchemphys.2017.11.055>.

- [22] Y. Du *et al.*, “Ameliorating structural and electrochemical properties of traditional polydioxolane electrolytes via integrated design of ultra-stable network for solid-state batteries,” *Energy Storage Materials*, vol. 56, pp. 310–318, Feb. 2023, doi: <https://doi.org/10.1016/j.ensm.2023.01.017>.
- [23] B. Halder, M. G. Mohamed, S.-W. Kuo, and P. Elumalai, “Review on composite polymer electrolyte using PVDF-HFP for solid-state lithium-ion battery,” *Materials Today Chemistry*, vol. 36, p. 101926, Jan. 2024, doi: <https://doi.org/10.1016/j.mtchem.2024.101926>.
- [24] J. Zhang *et al.*, “Polymer-in-salt electrolyte enables ultrahigh ionic conductivity for advanced solid-state lithium metal batteries,” *Energy Storage Materials*, vol. 54, pp. 440–449, Jan. 2023, doi: <https://doi.org/10.1016/j.ensm.2022.10.055>.
- [25] S.-Y. Du, G.-X. Ren, N. Zhang, and X.-S. Liu, “High-Performance Poly(vinylidene fluoride-hexafluoropropylene)-Based Composite Electrolytes with Excellent Interfacial Compatibility for Room-Temperature All-Solid-State Lithium Metal Batteries,” *ACS Omega*, vol. 7, no. 23, pp. 19631–19639, May 2022, doi: <https://doi.org/10.1021/acsomega.2c01338>.
- [26] K. Pożyczka, M. Marzantowicz, J.R. Dygas, and F. Krok, “IONIC CONDUCTIVITY AND LITHIUM TRANSFERENCE NUMBER OF POLY(ETHYLENE OXIDE):LiTFSI SYSTEM,” *Electrochimica Acta*, vol. 227, pp. 127–135, Feb. 2017, doi: <https://doi.org/10.1016/j.electacta.2016.12.172>.
- [27] Y.-P. Yang *et al.*, “Thermal Stability Analysis of Lithium-Ion Battery Electrolytes Based on Lithium Bis(trifluoromethanesulfonyl)imide-Lithium Difluoro(oxalato)Borate Dual-Salt,” *Polymers*, vol. 13, no. 5, p. 707, Feb. 2021, doi: <https://doi.org/10.3390/polym13050707>.
- [28] L. Zurita, “Ionic Conductivity, Li<sup>+</sup> Transference Number, and Diffusion Coefficient of a Solid-State Electrolyte Composite,” *Reviews, Analyses, and Instructional Studies in Electrochemistry (RAISE)*, vol. 1, no. 1, May 2024, doi: <https://doi.org/10.70163/2997-8947.1005>.
- [29] J. Chidiac, L. Timperman, and M. Anouti, “Physical properties and compatibility with graphite and lithium metal anodes of non-flammable deep eutectic solvent as a safe electrolyte for high temperature Li-ion batteries,” *Electrochimica Acta*, vol. 408, p. 139944, Mar. 2022, doi: <https://doi.org/10.1016/j.electacta.2022.139944>.
- [30] S. Zou *et al.*, “In-situ polymerization of solid-state polymer electrolytes for lithium metal batteries: a review,” *Energy & Environmental Science*, vol. 17, no. 13, pp. 4426–4460, Jan. 2024, doi: <https://doi.org/10.1039/d4ee00822g>.
- [31] Y. Liao, J. Kong, T. Hou, Z. Huang, Y. Han, and H. Xu, “Quasi-solid-state sulfur cathode with ultralean electrolyte via in situ polymerization,” *Energy Storage Materials*, Aug. 23, 2024. Available: <https://doi.org/10.1016/j.ensm.2024.103744>. [Accessed: Jul. 29, 2024]
- [32] Q. Zhu, C. Ye, and D. Mao, “Solid-State Electrolytes for Lithium–Sulfur Batteries: Challenges, Progress, and Strategies,” *Nanomaterials*, vol. 12, no. 20, p. 3612, Jan. 2022, doi:

- <https://doi.org/10.3390/nano12203612>. Available: <https://www.mdpi.com/2079-4991/12/20/3612>. [Accessed: Jan. 21, 2023]
- [33] J. Zhang *et al.*, “A Fully Amorphous, Dynamic Cross-Linked Polymer Electrolyte for Lithium-Sulfur Batteries Operating at Subzero-Temperatures,” *Angewandte Chemie International Edition*, vol. 63, no. 5, Dec. 2023, doi: <https://doi.org/10.1002/anie.202316087>
- [34] L. Hu *et al.*, “In Situ Polymerization Bi-Functional Gel Polymer Electrolyte for High Performance Quasi-Solid-State Lithium–Sulfur Batteries,” *Small*, vol. 20, no. 42, Jun. 2024, doi: <https://doi.org/10.1002/sml.202402862>
- [35] Y. Liao, J. Kong, T. Hou, Z. Huang, Y. Han, and H. Xu, “Quasi-solid-state sulfur cathode with ultralean electrolyte via in situ polymerization,” *Energy Storage Materials*, Aug. 23, 2024. Available: <https://doi.org/10.1016/j.ensm.2024.103744>. [Accessed: Jul. 29, 2024]
- [36] Z. Wang *et al.*, “Towards durable practical lithium–metal batteries: advancing the feasibility of poly-DOL-based quasi-solid-state electrolytes via a novel nitrate-based additive,” *Energy & Environmental Science*, vol. 16, no. 9, pp. 4084–4092, Jan. 2023, doi: <https://doi.org/10.1039/d3ee02020g>.
- [37] Ammaiyappan Anbunathan *et al.*, “Advanced quasi-solid-state lithium-sulfur batteries: A high-performance flexible LiTa<sub>2</sub>PO<sub>8</sub>-based hybrid solid electrolyte membrane with enhanced safety and efficiency,” *Journal of Energy Storage*, vol. 93, pp. 112294–112294, Jun. 2024, doi: <https://doi.org/10.1016/j.est.2024.112294>
- [38] Y. Pang, Z. Liu, and C. Shang, “The construction of quasi-solid state electrolyte with introduction of Li<sub>6.4</sub>La<sub>3</sub>Zr<sub>1.4</sub>Ta<sub>0.6</sub>O<sub>12</sub> to suppress lithium polysulfides’ shuttle effect in Li-S batteries,” *Materials Letters*, vol. 336, pp. 133874–133874, Jan. 2023, doi: <https://doi.org/10.1016/j.matlet.2023.133874>
- [39] M. Wei *et al.*, “Flexible ionic liquid aided ‘LAGP in PVDF’ quasi-solid-state electrolyte for high performance and stable Li metal batteries,” *International Journal of Hydrogen Energy*, vol. 79, pp. 1278–1288, Jul. 2024, doi: <https://doi.org/10.1016/j.ijhydene.2024.07.104>
- [40] Yuhang. Shan, Libo. Li, and Xueying. Yang, “Solid-State Polymer Electrolyte Solves the Transfer of Lithium Ions between the Solid–Solid Interface of the Electrode and the Electrolyte in Lithium–Sulfur and Lithium-Ion Batteries,” *ACS Applied Energy Materials*, vol. 4, no. 5, pp. 5101–5112, Apr. 2021, doi: <https://doi.org/10.1021/acsaem.1c00658>
- [41] Y. Yuan *et al.*, “Ionic liquid assisted quasi-solid-state polymer electrolyte for rechargeable lithium metal batteries operating at room temperature,” *Electrochimica Acta*, vol. 440, p. 141753, Feb. 2023, doi: <https://doi.org/10.1016/j.electacta.2022.141753>
- [42] K.-W. Lee, S.-M. Yeh, K.-H. Ni, and C.-C. Li, “Enhancing electrochemical performance of solid-state Li-ion batteries with composite electrolytes of fibrous LLZTO and PVDF-HFP: The role of LLZTO fiber diameter,” *Journal of Energy Storage*, vol. 74, p. 109531, Dec. 2023, doi: <https://doi.org/10.1016/j.est.2023.109531>.

- [43] Y. Gu, F. Liu, and G. Liu, "Preparation of new composite electrolytes for solid-state lithium rechargeable batteries by compounding LiTFSI, PVDF-HFP and LLZTO," *International Journal of Electrochemical Science*, vol. 15, no. 12, pp. 11986–11996, Dec. 2020, doi: <https://doi.org/10.20964/2020.12.65>.
- [44] J. Cai, T. Liu, C. Liu, and G. Liu, "PVDF-HFP/LiTFSI based composite solid state electrolyte with different micromorphology of Li<sub>6.25</sub>Ga<sub>0.25</sub>La<sub>3</sub>Zr<sub>2</sub>O<sub>12</sub> doping," *Journal of Alloys and Compounds*, vol. 968, p. 171872, Dec. 2023, doi: <https://doi.org/10.1016/j.jallcom.2023.171872>.
- [45] M. Kumar, "Phase-Inversion - an overview | ScienceDirect Topics," *www.sciencedirect.com*. Available: <https://www.sciencedirect.com/topics/engineering/phase-inversion>
- [46] S. Kumar, "Electrospinning - an Overview | ScienceDirect Topics," *www.sciencedirect.com*. Available: <https://www.sciencedirect.com/topics/materials-science/electrospinning>
- [47] L. Bi *et al.*, "Sulfhydryl-functionalized COF-based electrolyte strengthens chemical affinity toward polysulfides in quasi-solid-state Li-S batteries," *Carbon Energy*, Apr. 2024, doi: <https://doi.org/10.1002/cey2.544>
- [48] Pavithra Murugavel Shanthi, Prashanth Jampani Hanumantha, T. Toledo, Bharat Gattu, and P. N. Kumta, "Novel Composite Polymer Electrolytes of PVdF-HFP Derived by Electrospinning with Enhanced Li-Ion Conductivities for Rechargeable Lithium–Sulfur Batteries," *ACS applied energy materials*, vol. 1, no. 2, pp. 483–494, Jan. 2018, doi: <https://doi.org/10.1021/acsaem.7b00094>.
- [49] Y. Nikodimos *et al.*, "Al–Sc dual-doped LiGe<sub>2</sub>(PO<sub>4</sub>)<sub>3</sub> – a NASICON-type solid electrolyte with improved ionic conductivity," *Journal of Materials Chemistry A*, vol. 8, no. 22, pp. 11302–11313, Jun. 2020, doi: <https://doi.org/10.1039/D0TA00517G>.
- [50] R. Chen, W. Qu, X. Guo, L. Li, and F. Wu, "The pursuit of solid-state electrolytes for lithium batteries: from comprehensive insight to emerging horizons," *Materials Horizons*, vol. 3, no. 6, pp. 487–516, 2016, doi: <https://doi.org/10.1039/c6mh00218h>
- [51] R. Das and A. Chanda, "Fabrication and Properties of Spin-Coated Polymer Films," *Nano-size Polymers*, pp. 283–306, 2016, doi: [https://doi.org/10.1007/978-3-319-39715-3\\_10](https://doi.org/10.1007/978-3-319-39715-3_10).
- [52] L. Chen *et al.*, "Tailored Organic Cathode Material with Multi-Active Site and Compatible Groups for Stable Quasi-Solid-State Lithium–Organic Batteries," *Advanced Functional Materials*, vol. 32, no. 49, Oct. 2022, doi: <https://doi.org/10.1002/adfm.202209848>.
- [53] L. M. McGrath, J. Jones, E. Carey, and J. F. Rohan, "Ionic Liquid Based Polymer Gel Electrolytes for Use with Germanium Thin Film Anodes in Lithium Ion Batteries," *ChemistryOpen*, vol. 8, no. 12, pp. 1429–1436, Dec. 2019, doi: <https://doi.org/10.1002/open.201900313>.
- [54] R. Gonçalves *et al.*, "Solid polymer electrolytes based on lithium bis(trifluoromethanesulfonyl)imide/poly(vinylidene fluoride -co-hexafluoropropylene) for safer rechargeable lithium-ion batteries," *Sustainable Materials and Technologies*, vol. 21, p. e00104, Sep. 2019, doi: <https://doi.org/10.1016/j.susmat.2019.e00104>.